ASSESSING WITHIN-TREE VARIATION IN WOOD PROPERTIES OF LOBLOLLY PINE USING NONDESTRUCTIVE TECHNIQUES

by

SEYEDMOHAMAD NABAVI

(Under the Direction of Joseph Dahlen)

ABSTRACT

The objective of this study was to assess loblolly pine fiber properties within-tree variation. We determined fiber properties using fiber analyzer in conjunction with near-infrared spectroscopy (NIRS). Diffuse reflectance NIR spectra were collected from samples, age 19-31 acquired from across the Southeast in 10-mm radial sections from pith to bark. A subset of the samples were selected based on their NIR spectra uniqueness, macerated, and the fiber properties determined. Calibration models developed for fiber length were strong (R^2=0.88, SECV=265-µm, RPD=2.9). However calibrations for fiber width were moderate (R^2=0.48, SECV=1.99-µm, RPD=1.40). The calibrations were checked with a prediction set, and their performance was again strong for fiber length (R^2=0.84, SEP=0.261-mm, RPD=2.50) and moderate for fiber width (R^2=0.49, SEP=0.0018-mm, RPD=1.39). Within-tree variation of fiber length shows that it is low at the base of the stem and increases with height in the butt log. Fiber length increases from pith to bark, and the rate of change occurs at a faster pace at higher heights than near the stem base. Fiber width follows a similar trend to fiber length.

INDEX WORDS: fiber length, intensive management, near-infrared spectroscopy, pulp and paper, southern pine, wood quality

ASSESSING WITHIN-TREE VARIATION IN WOOD PROPERTIES OF LOBLOLLY PINE USING NONDESTRUCTIVE TECHNIQUES

by

SEYEDMOHAMAD NABAVI

BSC, University of Tehran, 2007

MSC, University of Tehran, 2010

A Thesis Submitted to the Graduate Faculty of The University of Georgia in Partial Fulfillment of the Requirements for the Degree

MASTER OF SCIENCE

ATHENS, GEORGIA

2016

ASSESSING WITHIN-TREE VARIATION IN WOOD PROPERTIES OF

LOBLOLLY PINE USING NONDESTRUCTIVE TECHNIQUES

by

SEYEDMOHAMAD NABAVI

Major Professor: Joseph Dahlen
Committee:

Kamal J.K. Gandhi
Michael Kane
Cristian Montes

Electronic Version Approved:

Suzanne Barbour
Dean of the Graduate School
The University of Georgia
December 2016

DEDICATION

I dedicate this thesis to the people in my life, without whom this endeavor would not have been possible. I would like to thank my father and mother, Kazem Nabavi and Najme Gholipour, for instilling in me a great work ethic and a passion for achieving my goals.

ACKNOWLEDGEMENTS

I would like to thank Warnell Warnell School of Forestry and Natural Resources without whose funding, this thesis would not have been possible. I would also like to thank The Wood Quality Consortium for funding and support of this project.

I would also like to thank my committee for their dedication and guidance towards the completion of this thesis. Thank you Dr. Dahlen, your encouragement and foresight allowed me to pursue this project, thank you Dr. Kane, for your dedication and commitment to research at Warnell, thank you Drs. Gandhi and Dr. Montes for your passion for students and seeing them succeed. I would also like to acknowledge Bryan Simmons and Rajesh Bitsa for their assistance with setting up instruments and helping to prepare and test samples.

TABLE OF CONTENTS

LIST OF TABLES

LIST OF FIGURES

CHAPTER 1

INTRODUCTION

Purpose of the study

The goal of this study is to assess the within-tree tracheid morphological characteristic variation of plantation-grown loblolly pine. Because of the influence of cambial age, tracheid morphology varies from pith to bark and in height (stump to tip) within a tree. Tracheid morphology plays a major role in determining pulp and paper properties and strongly influences product properties such as tear and burst strength, and it also impacts product processing. Recently intensive forest management practices have been used to increase tree growth rate which can negatively affect wood quality. This study establishes baseline information on fiber properties to better understand how fiber properties vary within plantation grown loblolly pine.

How the study is original

In the present study, loblolly pine (*Pinus taeda*) trees, age 19-31 from 109 plantations across the southeastern United States were examined for fiber properties. Plantations selected for sampling were planted with at least 1,235 trees per hectare and contained at least 617 trees per hectare after thinning. These stands were conventionally managed, which means that except for phosphorus deficient sites, they received no intensive management practices such as chemical competition control or fertilization. A total of 109 plantations and 150 trees were examined, and 1,842 disks were collected from within the trees. A pith to bark radial strip was cut from each disk (a total 1,842 radial strips). Each radial strip was then segmented into 10-mm sections from pith to bark to examine the influence of cambial age on fiber properties. Each disk had approximately 6 10-mm sections (total 11,482 10-mm sections). Macerating 11,482 10-mm sections was not feasible given time and budget constraints, so we scanned the samples using a near-infrared spectrometer, and then used the duplex sample selection method to pick 1,152 10-mm sections samples that had the most unique near-infrared spectra. The unique samples were macerated and their fiber properties measured. This study is one of the most comprehensive studies done in the United States that examined the within-tree variation in fiber properties of plantation loblolly pine.

CHAPTER 2

LITERATURE REVIEW

Loblolly pine

The Southeastern United States supplies over half of the total wood used in the U.S. and 16% of the wood used worldwide (Wear and Greis 2002, Zhao et al. 2011). Raw material demand is increasing, resulting in increased pressure on industrial forests to maximize the volume produced per hectare from forests (Zhao et al. 2011). Loblolly pine (*Pinus taeda*) is planted on more than 13.4 million hectares of forest land (Schultz 1997). A fast growth rate and the ability to survive on a broad range of sites, along with its suitability for a variety of uses has made loblolly pine the most common and commercially important species in the Southeast (Zhao et al. 2011). Loblolly pine stands can achieve high growth rates, for example, research trials have demonstrated growth rates of 29.4 m^3/ha per year (Borders and Bailey 2001). However, as wood growth increases concerns regarding the suitability of the resulting wood to make products also increase (White et al. 2009). Loblolly pine is used in the pulp and paper, residential construction, utility poles, composites, and energy markets (Gaby 1985).

Southern pine is the species group which is composed of longleaf pine (*Pinus palustris*), shortleaf pine (*Pinus echinata*), loblolly pine (*Pinus taeda*), and slash pine (*Pinus elliotti*) (Gaby 1985). These four major pines are the main source of softwood products in the United States (Stanturf et al. 2012). The geographic range of these species overlap and include the upper areas of the South Atlantic States across the southern states to Texas and Oklahoma. The southern pines have similar looking wood which is difficult to differentiate between species (Panshin and DeZeeuw 1980, Hoadley 1990, Schultz 1999). The wood for the southern pines is strong, dries fast, treats easily with chemicals, and works moderately hard with tools (Gaby 1985).

Wood quality

Wood quality refers to a combination of anatomical, chemical, physical and mechanical characteristics of wood. The term "wood quality" is dependent on the desired product quality and thus an understanding of what defines quality can differ between different wood products (Briggs and Smith 1986). Therefore, the emphasis is placed on the wood properties that have positive correlations with specific end products (Antony et al. 2013). For solid wood products, common wood properties that influence wood quality include specific gravity (SG), microfibril angle (MFA), modulus of elasticity (MOE) or stiffness, and modulus of rupture (MOR) or strength (Antony 2010). For pulp and paper products, pulp yield, fiber length, cell wall thickness, fiber coarseness, and fiber width alongside SG and microfibril angle (MFA) are common wood quality indicators (van Leeuwen et al. 2011).

Density or specific gravity (SG) is the amount of woody material in a given volume of wood. Specific gravity has a strong correlation with the strength of wood, as has been linked to the cellulose content of wood (Wang 2003, Murphy 2008, White et al. 2009). Specific gravity is dependent upon the ratio of earlywood to latewood in an annual ring and the thickness of the fiber walls. Wood with higher SG typically has longer tracheids, which produces Kraft sack papers with higher tear resistance (Smook 2002). On the other hand, wood which has a lower SG will have thinner walls and generally shorter tracheids, wider MFA and as a result, produces paper with excellent print quality and sheet smoothness, but lower tensile, fold, tear, and opacity (Smook 2002). While SG is positively correlated with many wood properties, there are many other important properties including MFA, stiffness, strength, fiber length, and cell wall thickness that are critical for various industrial processes and products and are more important than SG depending on the product (Inagaki et al. 2012).

Microfibril angle is defined as the angle between microfibrils in the S2 layer of the cell wall and the longitudinal axis of the cell (Sewell et al. 2000). Between 75-85% of the total cell wall thickness is made of the S2 layer and thus the MFA of the S2 layer tends to dominate (Donaldson 2008). Microfibril angle has a strong influence on the MOE, MOR and dimensional stability of wood and is an important indicator of the sawn timber's quality (Macdonald and Hubert 2002, Auty et al. 2013). Tensile strength and MOE of pulp are functions of MFA as well, and fibers with lower MFA will produce stronger and stiffer pulp (Donaldson 2008). In loblolly pine, MFA was found to be a major affecting factor of hand-sheet tensile strength, stretch, modulus of elasticity, stiffness, and hygroexpansivity of unbleached Kraft pulp (Courchene et al. 2006).

Modulus of elasticity and MOR are the two most important wood properties when wood is used in structural applications. Modulus of elasticity is a material's tendency to deform elastically under pressure and is referred to as the material stiffness. On the other hand, MOR is a measure of a specimen's strength at rupture, which is known as strength. Since these properties will determine the end use of the wood for structural products, recognizing them is necessary for depicting wood quality for structural products (Antony et al. 2011).

Tracheid morphological properties include fiber length, fiber width, cell perimeter and cell wall thickness and these anatomical properties strongly influence pulp and paper properties and products (Zobel and Van Buijtenen 1989, McKenzie 1994, Smook 2002, Pulkkinen et al. 2006). The fiber length is the length of the wood cell and affects the tensile strength, breaking strain and fracture toughness of dry paper, and is especially important for wet web strength (Niskanen 1998, van Leeuwen et al. 2011). The cell perimeter, which is correlated with wood density and cellulose content, can be calculated by multiplying of sum of tangential and radial cell diameter by two (Stokke and Groom 2008). Tangential and radial cell diameter can be measured on cross-sections using image analysis tools (Lundgren 2004). Water transport and mechanical support are two important properties which are affected by cell perimeter (van Leeuwen et al. 2011). Fiber width and cell wall thickness have a strong influence on plasticity and resistance to the processing of fibers and affect fiber propensity for collapsing in the papermaking process (Paavilainen 1993). Fibers with thinner walls collapse more promptly and have stronger bonding within the paper and thus the sheet will be denser, stronger and smoother (Kibblewhite 1989). If a sheet with high bulk is needed, fibers must have thicker walls so they will resist collapse, but such fibers will result in a sheet with low opacity (Seth et al. 1996). Moreover, resistance to collapsing will happen if fibers have a small lumen perimeter (Hoyland et al. 1976). Fiber with a larger perimeter and thinner walls produce denser, stronger, and smoother paper (Wang and Aitken 2001, van Leeuwen et al. 2011). The ratio of cell wall mass to cell unit length is defined as cell coarseness which is closely correlated with drought resilience (Gartner 2008). Strength and stiffness of pulp are highly influenced by cell coarseness (Via et al. 2005). With a given fiber diameter, coarser fibers have thicker cell walls. Such fibers are stiffer and more rigid and resist collapse during paper making. Thus, these coarser fibers produce sheets that are bulkier, more porous and rougher than sheets produced from less coarse fibers (Muneri and Raymond 2001). As wood density decreases, the cell coarseness and pulp yield decrease, while the quality of paper increases (van Leeuwen et al. 2011).

Wood and fiber properties vary within-tree (Megraw 1985, Wang and Aitken 2001) and thus an understanding of the variation in wood properties is necessary for the determination and optimization of proper production procedures (Antony et al. 2011). Due to the within-tree variation, within a batch of pulp, the morphological properties of fibers vary a great deal (Niskanen 1998). The variation within the stem changes from pith to bark (cambial age) and stump to tip (height), and thus fiber properties vary with corewood and outerwood and juvenile and mature wood (Burdon et al. 2004). Cell wall thickness, fiber width and fiber length increase from pith to bark (cambial age) (Wang and Aitken 2001). At a given cambial age, the fiber length is higher in the upper portion of the stem than in the lower part (4,000-µm length at the height of 20-m in a 41 years old tree and 1,000-µm length at the base of 41 years old tree) (Megraw 1985, Borch et al. 2001). Beside stump to tip and pith to bark variation, fiber characteristics vary within an annual ring based on earlywood and latewood (Borch et al. 2001). For example, cell perimeter gradually decreases from earlywood to latewood (van Leeuwen et al. 2011) and within a single fiber cell, wall thickness fluctuates significantly between 3.0 to 5.8-µm (Pulkkinen et al. 2006).

Within-tree variation of fiber length in *P. taeda* studied by researchers (Megraw 1985, Groom et al. 2002) revealed that fiber length is shortest near the pith (2,000-µm), and increase radially outward with age (4,000-µm). This trend applies to any given cross section regardless of height. The rate at which fiber length increases with age from the pith is slower at the base of the tree than at higher heights. Table 1 shows how wood properties change within-tree (from pith to bark and stump to tip) for multiple wood properties. The distribution of tracheid dimensions in *Sequoia sempervirens* and *S. giganteum* has been summarized (Bailey 1958). At ages 1, 10, 25, and 120, the distribution of tracheids is centered around 1,000-µm, 2,200-µm, 2,800-µm, and

4,500-µm, respectively. The change in wood properties from pith to bark, including tracheid length, was thought to be because of the size of the cambial initials in the vascular cambium (Lachenbruch et al. 2010). However, this assumption has been challenged recently and we now suspect that wood anatomy changes from pith to bark because of hydraulic and mechanical requirements (Lachenbruch et al. 2010).

Table 1. Within-tree variation of wood properties from pith to bark and stump to tip

Wood property	Pith to bark	Stump to tip	Source
Specific gravity	Increase	Decrease	(Megraw 1985, Antony et al. 2010)
Cell wall thickness	Increase	Decrease	(Wang and Aitken 2001, van Leeuwen et al. 2011)
Microfibril angle	Decrease	Decrease	(Jordan et al. 2006, Jordan et al. 2007)
Fiber length	Increase	Increase	(Megraw 1985, van Leeuwen et al. 2011)
Fiber width	Increase	Increase	(Lundqvist 2002, Wathén 2006)

Forest management influence on wood quality

Many studies have shown intensive forest management increases the growth rates in southern pine plantations (Borders and Bailey 2001, Haywood 2005). For example, thinning pine stands has been shown to increase growth rates of individual trees (Baldwin et al. 2000, Nilsson and Allen 2003). Fertilization and vegetation control have been shown to increase stand growth and increase average tree size (Zhao et al. 2011). Site preparation that improves soil conditions and control of competing vegetation can result in increased seedling survival and growth (Löf et al. 2012). As the planting density increases the stand basal area and stem volume increase as well, thus, the average diameter at breast height (DBH) decrease (Pienaar and Shiver 1993, Harms et al. 2000).

The negative effect of rapid tree growth on wood properties is a concern to the forest products industry. For instance, specific gravity has a high correlation with structural wood properties strength and yield and quality of pulp (White et al. 2009) and following fertilization a decrease in specific gravity has been reported (Zobel 1961, Love-Myers et al. 2010). Increasing the growth rate of pine plantations in the the early years of a rotation causes increases in the juvenile wood to mature wood ratio (Roth et al. 2007). Juvenile wood is less desirable because it has lower strength and stiffness, and has a higher MFA than mature wood (Cramer et al. 2005). Planting at wide spacing promotes rapid stem diameter growth resulting in more low specific gravity wood, and with increasing planting density, specific gravity is reduced (Clark et al. 2008).

Near-infrared spectroscopy

Traditional methods used to measure wood properties are time-consuming, expensive, and destructive. To feasibly analyze large numbers of samples, rapid and cost-effective methods are needed that can provide the information required for effective decision-making in the wood industry (Schimleck et al. 2003). Using near-infrared spectroscopy (NIRS) has several advantages over other instruments as it provides a rapid estimation of a variety of wood properties and is nondestructive (Mora 2009). The NIR region (700-2500 nm) is made up of harmonic and joining bands of the core stretching vibrations of O-H, N-H and C-H functional groups which contain chemical and physical information about a sample (Burns and Ciurczak 2007). The basis of reflectance NIR instrument is to measure the absorption of NIR light from the surface of a wood sample and compare the absorption to a reference material such as ceramic or Teflon. The absorption of light generates vibrations of chemical bonds in various components such as cellulose, lignin, and extractives in wood, which in turn causes bands in the NIR spectra (Figure 1). As these bands (700-2500 nm) are related to the different components of wood, changes in them reflect changes in wood characteristics (Mora 2009). Various types of samples can be analyzed successfully, for example when using this technique surface roughness does not have a significant impact and thus solid wood samples can be evaluated (Schimleck et al. 2005).

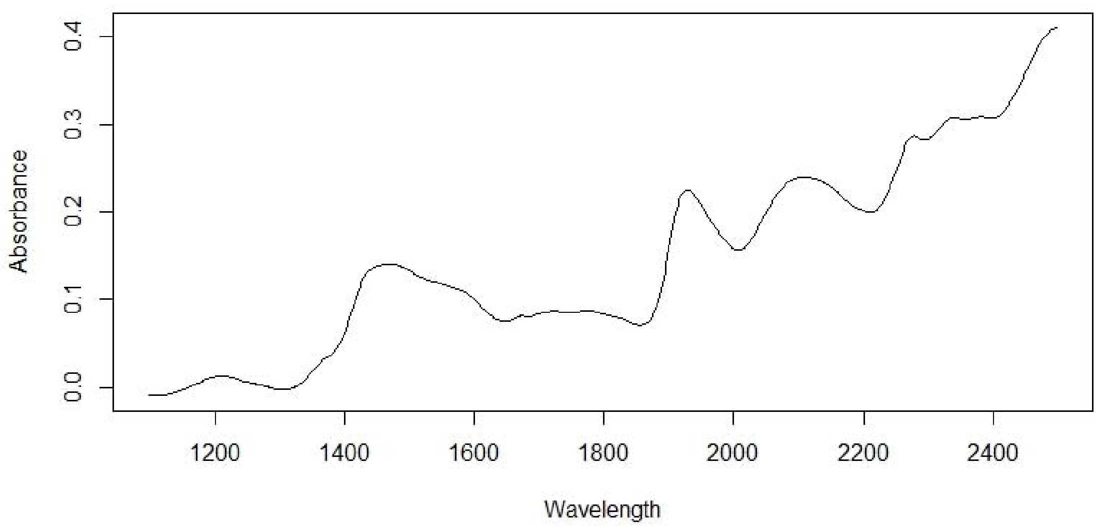

Figure 1. Typical NIR spectra for loblolly pine

The major disadvantage of NIRS is that it does not directly measure any wood properties. Thus the use of NIRS requires a calibration model to compare the NIR spectra to a reference method. The calibration models are developed using multivariate statistics which establish linear combinations of the spectral data which overcome the problem of multiple overlapping peaks in NIR spectra as well as summarizing the significant amount of information contained in the NIR spectra (Alves et al. 2007). The two main types of multivariate analysis used are principal component analysis (PCA) and partial least square (PLS) regression (Ziegel 2004). These methods reduce the data and cause the resulting components to be more directly related to the variability in the dependent variable (Ziegel 2004). For example, Alves et al. (2007) used PLS regression to create a model to predict pulp characteristics based on NIR spectra and found that NIR spectroscopy can be used as an appropriate tool to predict pulp characteristics with unknown Kappa numbers.

Recent findings have shown that near-infrared spectroscopy can estimate many wood properties including SG, MFA and fiber length (Schimleck et al. 2001, Via 2004, Jones et al. 2005, Via et al. 2005). Several studies have shown that NIR spectroscopy can be successfully used to estimate a broad range of wood properties including chemical, anatomical, physical and mechanical properties of wood (Hauksson et al. 2001, Schimleck and French 2002, Via et al. 2003, Schimleck et al. 2005, Jones et al. 2006). Earlier studies focused on chemical components such as cellulose and lignin (Raymond and Schimleck 2002, Hodge and Woodbridge 2004, Yeh et al. 2004, Jones et al. 2006) or properties directly related to such components, for example, pulp yield (Schimleck and French 2002, Schimleck et al. 2006). Recently research has broadened to include physical and mechanical properties as well (Gindl et al. 2001, Kelley et al. 2004, Tsuchikawa 2007, Fujimoto et al. 2008, Tsuchikawa and Schwanninger 2013).

Several studies have utilized NIRS to analyze wood property variation from pith to bark (Pot et al. 2002, Jones et al. 2005, Jones 2006, Jones et al. 2008). The pith region has shown significant variation in NIRS which leads to inaccuracies in the predicted values (Jones et al. 2006, Jones et al. 2008). Meder et al. (2011) used NIRS to develop a radial profile of chemistry and MFA from pith to bark of radiata pine and found that in the pith zone there was a mismatch between NIR-predicted and SilviScan determined MFA. Ivković et al. (2009) measured the stiffness, strength, and shrinkage of juvenile wood, pith to bark radial strips of radiata pine and compared the properties to MFA measured by SilviScan and found significant variation in the pith zone of samples. The inaccuracy of the models near the pith may be due to the variability in the pith cell types which is impacting the NIR prediction, or it could be due to the estimation error of SilviScan MFA near the pith (Verrill et al. 2011).

Schimleck et al. (2004) analyzed 40 radial strips of *P. taeda* samples and found R^2 of 0.88 between measured and NIR-predicted fiber length with standard error perdition (SEP) of 250-µm. Via et al. (2005) used NIR to analyze longleaf pine (*P. palustris*) for fiber length and found that regardless of age, the model could predict fiber length well (R^2=0.72). Inagaki et al. (2012) examined the feasibility of using NIR for non-destructive evaluation of fiber length in 50 samples of *Eucalyptus camaldulensis*. They obtained very high R^2 (R^2=0.98, SEP=15-µm) and ratio of performance to deviation (RPD) of 3.5 for fiber length. The good model statistics acquired in these studies suggests that NIR is a suitable tool for rapid prediction of fiber length.

Objective

The main aim of this research is to assess the within-tree variation of loblolly pine fiber properties. The samples were collected from different regions and from different areas within the trees which have variable wood properties (such as MFA and density) (Mora and Schimleck 2009). This study can improve understanding of within-tree fiber property variation in planted loblolly pine. We aimed to develop a model using NIRS to predict tracheid length and width from loblolly pine samples. Conclusions from this study may be helpful and meaningful for the forest product industry along with forest managers and foresters across loblolly pine's natural habitat. Knowledge about fiber properties variation could potentially help the forest product sector have a better picture about adjustments needed for each product and the manufacturing process. Previous researchers have shown that there is regional variation in some wood properties such as SG (Jordan et al. 2008), MOE, and MOR (Antony et al. 2011). Additional work on tracheid length may reveal similar variations in tracheid properties for loblolly pine.

CHAPTER 3

MATERIAL AND METHODS

Samples

We used samples collected from planted loblolly pine across the southeastern United States from the Wood Quality Consortium (WQC) baseline study (Jordan et al. 2008). These samples were collected with collaboration of the University of Georgia, the United States Department of Agriculture (USDA) Forest Service Southern Research Station and the forest industry. In this study, trees were 19 to 31 years old, tree heights ranged from 11.39 to 30.05-m and their diameter at breast height (DBH) ranged from 13.97 to 36.57-cm (Antony et al. 2010). These trees were sampled from 109 stands located in six geographical regions; 1) Southern Atlantic Coastal Plain, 2) Northern Atlantic Coastal Plain, 3) Upper Coastal Plain, 4) Piedmont, 5) Gulf Coastal Plain and 6) Hilly Coastal region. The stands did not have intensive fertilization (except in deficient phosphorus sites) or complete competition control. The plantations selected for sampling were planted with at least 1,235 trees per hectare and contained at least 617 trees per hectare following thinning. From each tree, 2.5-cm thick wood disks were extracted at 1.5-m intervals from the base of each tree up to a height of 2.5-cm top diameter. Radial 12.5×12.5-mm sections were obtained from the pith to bark. A total of 1,842 radial strips were collected from 1,842 disks, 150 trees, and 109 stands.

The samples were prepared to have square and rectangular sides using a belt sander. Each sample was marked into 10 mm sections from pith to bark on the tangential face, and the number of growth rings in each 10-mm section was recorded to allow for reconstruction of the tree by cambial age. Each sample was evaluated for cases where a knot, blue stain or another defect that would negatively impact the NIR spectra was present; all 10-mm sections presented here were defect-free.

Near-infrared spectroscopy

We used a FOSS NIRSystems Model 5000 scanning spectrophotometer (FOSS NIRSystems, Inc., Laurel, MD) with a diffuse reflectance static module to scan the wood samples on the radial face. Samples were conditioned and scanned in a 20° C and 40% relative humidity controlled environment room. The NIR window on the static module was 30-mm in diameter. A Teflon mask with a window measuring 5-mm × 10-mm was used to concentrate the NIR light on a constant area of each sample in 10-mm increments from bark to pith. This instrument collected the spectra at 2-nm intervals over the wavelength range from 1100-nm to 2500-nm. The instrument reference was a ceramic standard. Fifty scans were done for each 10-mm section, and these scans were averaged by the device software to give a single spectrum per section. The samples were scanned from pith to bark, and thus longer samples had more individual scans than shorter samples. Since automation of scanning samples will increase the number of samples scanned daily, an autosampler consisting of a servo motor and controller, and a linear screw drive was used to move samples automatically from pith to bark at 10-mm intervals.

Near-infrared scpectroscopy statistical analysis

The end-goal of NIRS is to develop a calibration model to predict the properties of new specimens. It is desirable to develop the calibration model using a large number of samples grown under various conditions (Jones et al. 2005). In this study, we scanned 1,842 samples from bark to pith using NIRS with each sample having approximately six scans. The 1,842 samples produced 11,444 NIR spectra. Then we split our data into three sets, a calibration set which was used to develop the calibration model, a prediction set which was used to assess the model performance and validate if the model worked, and a second prediction set where can be used for predicting the properties of new samples where refrence data was not collected, such as measuring fiber length. The identification of appropriate samples for the calibration model is sometimes done randomly, however, it is desirable to split the samples based on their spectral characteristics (Mora and Schimleck 2008). The sample selection was conducted using principle component analysis (PCA) and the duplex method (modified Kennard-Stone method) (Snee 1977). By selecting the unique samples between all possible pairs of samples, based on the Mahalanobis distance, the duplex algorithm splits the sample population into calibration and validation sets. First, all of the samples were allocated to a list of samples, then the sample with the longest distance inside the list was selected and moved to the calibration set. Next, the sample in the list with the furthest distance was chosen and transferred to the validation set. The process of selecting pairs of samples with the furthest distance, and assigning them to either calibration or validation sets continues until there is no sample left in the list (Mora and Schimleck 2008, Dahlen et al. 2016). Within the calibration and validation set, we then used the Kennard-Stone algorithm (Kennard and Stone 1969) to pick unique samples within each calibration and validation set for maceration using a similar procedure as the duplex method except there is not split between groups. The samples that were not selected for the calibration set or the validation set were placed in the prediction set. The breakdown of samples by region, by height within-tree, and those that were macerated, are shown in Table 2. The sample selection method was critical in reducing the number of the samples before maceration since macerating 11,444 specimens (11,444 10-mm sections) was not feasible. Also, by having the samples selected based on the spectra and not randomly by the calibration model, we likely improved the model performance since the variation in the spectra was considered when selecting samples. By using the duplex sample selection method, samples were split into calibration (576 samples) and validation (574 samples) sets (Stevens and Ramirez–Lopez 2014).

Following the sample selection procedure, the selected sections within each sample were marked and then cut into 10-mm sections using a razor blade. Each of these 10-mm sections was cataloged so they could be backtracked to a specific sample and height in a tree. These sections were used to measure specific gravity and fiber properties.

Table 2. Number of scanned and macerated samples from each region and height

	NIR scanned					Macerated
Region	Samples	10-mm sections	Heights			10-mm sections
			< 1-m	1-3.1-m	> 3.1-m	
North Atlantic	347	2,130	248	508	1,374	243
Piedmont	325	1,083	160	261	608	126
Upper Coastal Plain	196	1,397	189	304	904	125
South Atlantic	153	1,238	180	258	810	127
Hilly Coastal	273	1,943	273	442	1,228	181
Gulf Coastal Plain	548	3,637	462	859	2,646	350
Total	1,842	11,428	1,512	2,632	7,300	1,152

Specific gravity

Samples were weighed with the balance to measure the mass. The volume of the samples was measured using the water displacement method (Figure 2) (ASTM-D2395 2014). The samples were saturated with water for three days. After three days, the volume was measured using a 200-mL beaker containing water. The beaker was placed on the balance and tared. The sample was held below the water surface with a needle. It was completely submerged in the water without touching the sides of the beaker and care was taken so that the sample was fully submerged but not placed far below the water surface. After reaching the equilibrium, the samples volume was read accurately on balance as the mass of the displaced water (Figure 2). The SG was then calculated by dividing the mass of wood by the mass of the displaced water.

The specific gravity of wood is defined as the density of wood relative to the density of water, which is 1 g.cm^{-3} at 4.4°C and is unitless.

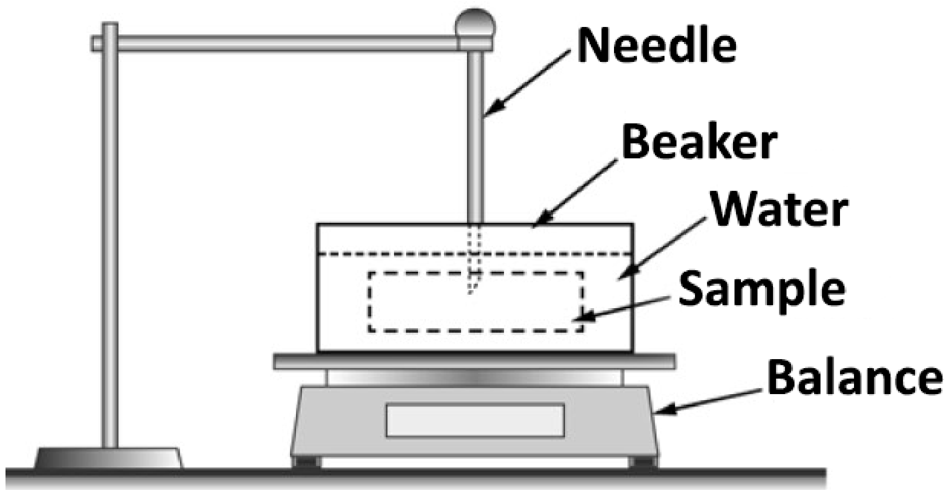

Figure 2. Sketch of apparatus used to measure volume of specimens (ASTM-D2395 2014)

Fiber properties

The samples were macerated to separate the fibers from the wood matrix. The 10-mm sections were cut into wood slivers using a razor blade, and the wood was boiled for 4 hours to soften the wood fibers before maceration. The samples were then macerated with 20-mL of 50% hydrogen peroxide, 30-mL of water, and 50-mL glacial acetic acid at 60°C for 48 hours (Franklin 1945) (Figure 3). After 48 hours the fibers were rinsed with approximately 1.9-L of water. The acidic spent pulping chemicals were neutralized with sodium carbonate. Image analysis of fibers is a reliable and efficient method for analyzing fiber length because human measurement via microscope is time-consuming (Pulkkinen et al. 2006). The macerated samples were analyzed using a TechPap MorFi Compact Fiber & Shive Analyzer (Techpap SAS, France) to assess the fiber properties. This equipment measured the number of fibers, frequency of fibers, fiber length, fiber width and other fiber properties using image analysis. For each sample, approximately 2,500 fibers were analyzed. The length-weighted fiber length and the width weighted fiber width were used for all calculations instead of the mean value because it better represents the actual fiber length by minimizing the effect of fines (Carvalho et al. 1997). Length-weighted fiber length is calculated by the following equation using the instrument's software:

$$(1)\ L_l = \frac{\sum_{n_i l_i}{}^2}{\sum_{n_i l_i}}$$

Where L_l is length-weighted fiber length, n_i is number of fibers in the *i*th class, and l_i is the mean length of the *i*th class (Carvalho et al. 1997). Width weighted fiber width was calculated, using the same equation but changing the length to width.

Figure 3. Maceration process; (1) samples being macerated (2) and fibers measured by MorFi fiber analyzer

Data analysis

The collected data was analyzed using the R statistical software (R Development Core Team 2016) RStudio interface (RStudio Team 2016), and the *prospectr* (Stevens and Ramirez–Lopez 2014), *chemometrics* (Filzmoser and Varmuza 2016), *pls* (Mevik et al. 2015), signal (Signal Developers 2013) and *rpart* (Therneau et al. 2015) packages in R. The NIR spectra were smoothed with a math pretreatment (second derivative), which has been used to improve the accuracy of the prediction performance in modeling wood properties by reducing spectra noise (Jones et al. 2005, Yang et al. 2016). The second derivatives were acquired from the untreated spectra using the Savitzky-Golay approach (Savitzky and Golay 1964), with left and right gaps of four nm to reduce noise within spectral data (Naes et al. 2002). The samples were selected using the duplex method in the *prospectr* package (Stevens and Ramirez–Lopez 2014) which has numerous pretreatment and the sample selection algorithms. Then PLS regression was used for the smoothed data to develop linear models to predict fiber properties of the samples (Mora and Schimleck 2008). Partial least square regression analysis can analyze strongly collinear and noisy data with numerous predictor variables while simultaneously modeling several responses variables. In other words, factors are mutually independent linear combinations of original descriptors. Latent variables are chosen in such a way as to provide maximum correlation with the dependent variable; thus, PLS models contains the smallest necessary number of factors (Höskuldsson 1988, Naes et al. 2002, Mora et al. 2008). In the application of the PLS algorithm, it is generally known that the spectral range and the number of PLS factors are critical parameters. The spectral range determines the location and quality of spectral information, and the number of PLS factors should be optimally selected to avoid overfitting (Chung et al. 2004). Calibrations were developed with four cross-validation segments taking into consideration a maximum of ten factors. The standard error of cross-validation (SECV) (determined from the residuals of each cross-validation phase), the root mean square error of cross-validation (RMSECV), the coefficient of determination of cross-validation (R^2), and the ratio of performance to deviation for the cross-validation (RPD_{cv}) were used to calculate the final number of factors and to assess calibration performance (Williams and Sobering 1993). The RPD_{cv} is determined as the ratio of the standard deviation of the reference data to the SECV. Determination of RPD_{cv} allows comparison of calibrations developed for different wood properties that have various data ranges and units; the higher the RPD_{cv}, more precisely the calibration describes the data (Granato and Ares 2013).

The performance of the calibrations is important to predict wood properties of an independent test sample (prediction set). The standard error of prediction (SEP) (determined from residuals of the predictions) was calculated and gives a measure of how well the calibration models predicts the parameters of interest for a set of samples not included in the calibration set. The predictive ability of the calibrations was assessed by the coefficient of determination (R_p^2) and calculating the RPD_p, which is similar to the RPD_{cv}, but uses the standard deviation of the prediction set reference data and the SEP (Mora and Schimleck 2008).

Within-tree variation in fiber properties was grouped based on the samples' height within the tree using visual inspection of the fitted curves. The fitted curves were constructed using fiber properties of disks and represent the longitudinal variation of fiber properties in a whole tree. These curves developed using smoothing spline which is a method of fitting a smooth curve to set of discrete and noisy observations using a spline function (Craven and Wahba 1978). The samples were divided into three different height categories; samples in the stump or butt area (below 1-m), samples between 1 to 3.1-m from the stump, and samples above 3.1-m.

CHAPTER 4

RESULTS AND DISCUSSION

The fiber properties of 2.9 million fibers were measured for this study. Fiber properties of the calibration and prediction data sets are presented in Table 3. The fiber length and fiber width data are highly variable which indicates the variability of these properties. Both data sets have similar summary statistics for each property. This similarity reflects that the duplex sample selection algorithm successfully selected calibration and prediction samples across the range of values using the NIR spectra information. The number of samples was approximately equally split into the calibration and prediction sets. The mean value for fiber length was 2,147-µm with a standard deviation of 648-µm in the calibration set, with a mean value of 2,221-µm and standard deviation of 649-µm in the prediction set. The average value for fiber width was 39.30-µm with a standard deviation of 2.80-µm in the calibration, with a mean value of 41.0-µm and standard deviation of 2.60-µm in the prediction set.

Table 3. Statistical summary of the calibration and prediction set for fiber length (µm) and fiber width (µm)

	Calibration (n=576)				Prediction (n=574)			
Property	Min	Max	Mean	Std	Min	Max	Mean	Std
Fiber length (µm)	1085	3997	2147	648	1101	3821	2221	649
Fiber width (µm)	33.0	46.0	39.30	2.80	32.0	47.0	41.0	2.60

Near-infrared models for fiber length and fiber width

A total of 576 NIR spectra were used for calibration development and a total of 574 spectra were used for the prediction set. The results of the calibration and their predictions for fiber length measured in the study by using the second derivative spectra are shown in Table 4. Seven factors were chosen for the calibration model. The tracheid length calibration gave R^2=0.88 with SECV= 265.5-µm. The calibration model, when applied to the prediction set, had R_p^2 similar to the R^2 found in the calibration set (R_p^2=0.83, SEP=261.5-µm). The fiber length RPDs for cross-validation and prediction were 2.93 and 2.50, respectively. As these RPDs are in-between screening (RPD ≥ 2.5) and quality control (RPD ≥ 5), the models are at least appropriate for screening in breeding programs (AACC 1999). The relationship between measured values and NIR fitted values for fiber length for calibration and prediction sets are shown in Figure 4.

Table 4. Fit statistics for the multiple heights NIR calibrations developed for fiber length (µm) and fiber width (µm)

	Calibration					Prediction		
Property	# factors	R^2	SEC	RMSECV	RPD_{cv}	R_p^2	SEP	RPD_p
Fiber length (µm)	7	0.88	220.8	265.5	2.93	0.84	261.5	2.50
Fiber width (µm)	7	0.48	1.99	2.33	1.40	0.49	1.85	1.39

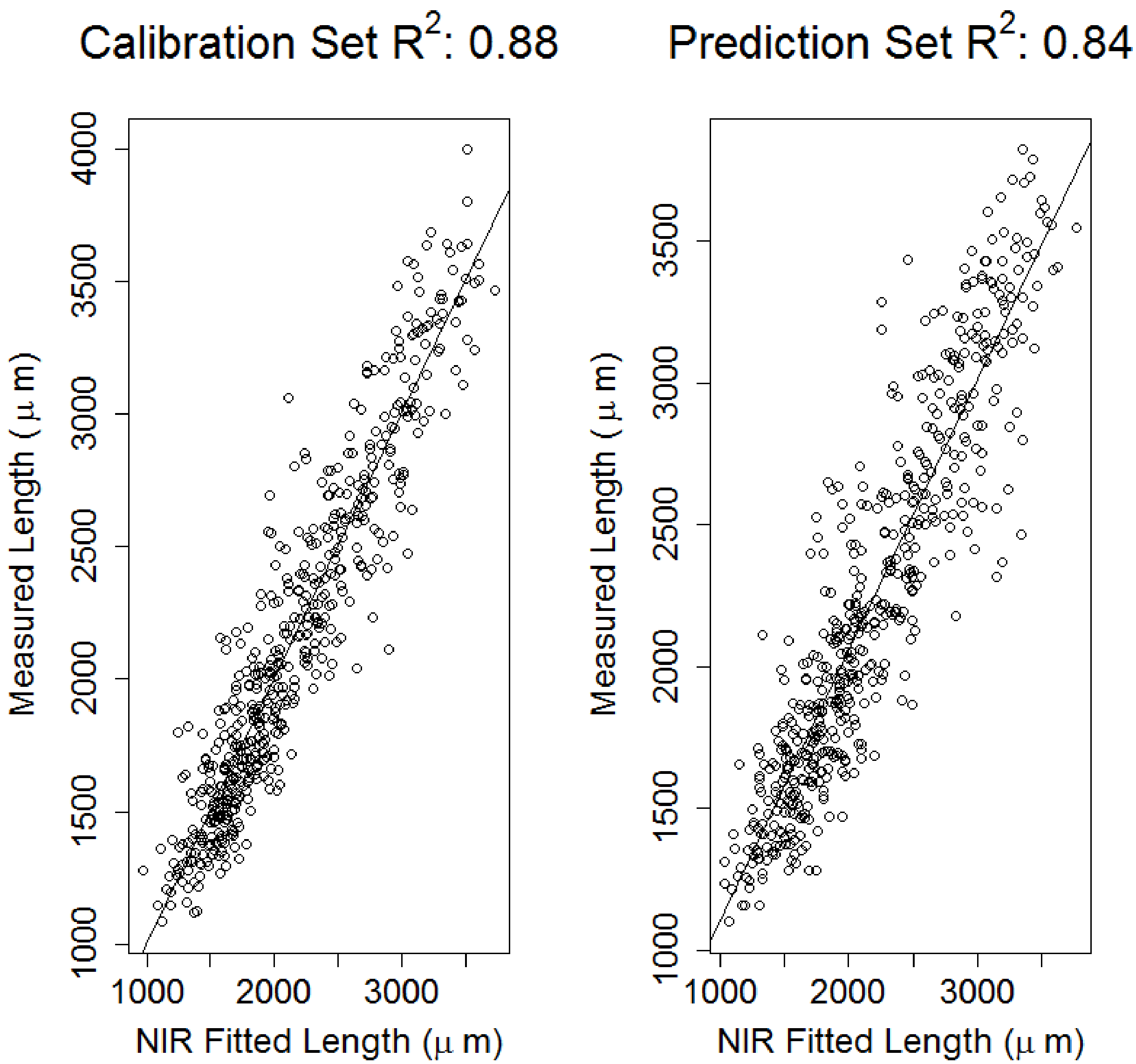

Figure 4. The relationship between measured values and NIR fitted values for fiber length (µm), for (left) calibration set and (right) prediction set.

For fiber width, seven factors were chosen for the calibration models. The relationship between measured values and NIR fitted values for fiber width for calibration and prediction set are presented in Figure 5. The fiber width calibration gave R^2=0.48 with SECV=2.33-µm. The prediction of fiber width had R_p^2 similar to R^2 (R_p^2=0.49, SEP=1.85-µm). The fiber width RPDs for cross-validation and prediction were 1.40 and 1.3, respectively. As these RPDs are below screening (RPD≥2.5), the models are not practical for screening purposes in breeding programs (AACC 1999).

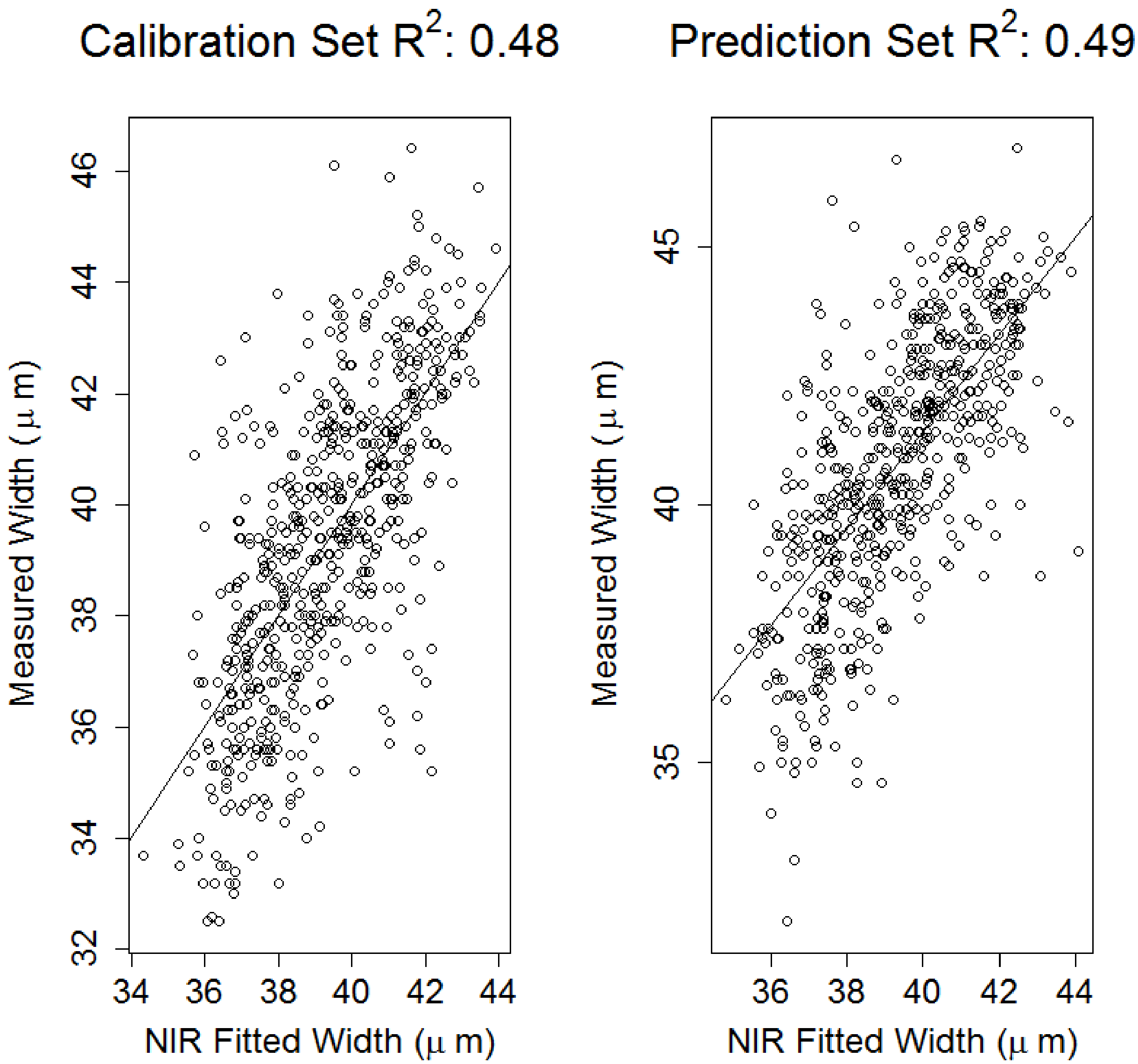

Figure 5. The relationship between measured values and NIR Fitted values for fiber width (µm), for (left) calibration set and (right) prediction set.

Calibrations developed for fiber length using diffuse reflectance NIR spectra collected in 10-mm sections showed strong calibration statistics (R_p^2=0.83, SEP=261.5-µm). These statistics indicated that NIR spectroscopy might be a useful tool for rapid estimation of fiber length in samples and the RPD_p for fiber length was sufficiently high to show that NIR prediction could be used for screening purposes.

The fiber length SEP in the current study of 265-µm was similar to that reported by Schimleck et al. (2004) (R_p^2=0.86, SEP=250-µm). The current study evaluated a considerably larger number of samples (1,152 samples vs. 40 samples) and thus included variation in site, climate, genetics, and soil type. The calibration statistics reported here (R_p^2=0.83, SEP=261.5-µm) are stronger than those reported by Hauksson et al. (2001) for milled wood (R_p^2=0.52). Using longleaf pine and a smaller calibration set (n=300) Via et al. (2005) showed weaker calibration statistics (R_p^2=0.72) for solid wood. An important factor in the success of this work was that NIR spectra were collected from the same section of wood that was later used for fiber length analysis. In comparison, Via et al. (2005) used wood for fiber analysis that was obtained from a larger area than their NIR spectra were collected from, leading to the unnecessary variation that probably had a negative effect on the fiber length calibrations they reported Schimleck and Evans (2004) used 32 cores of *P. radiata* to demonstrate the ability of NIR spectroscopy to estimate tracheid morphological characteristics and reported R_p^2 of 0.91 and 0.89 for coarseness and wall thickness, respectively. Jones et al. (2005) used a sample set (n=119) of *P. taeda* grown on 14 sites to study tracheid morphological and found that, although tracheid morphological characteristics showed a slight reduction in calibration R^2 (0.80 for coarseness and 0.84 for wall thickness) and increase in calibration error (41.47-µg/m for coarseness and

0.26-µm for wall thickness), tracheid morphological properties continued to provide good relationships.

Fiber width model performance was not strong as for fiber length (R_p^2=0.49, SEP=1.85-µm). The RPD_p value for fiber length was 2.5 whereas the RPD_p value for fiber width was 1.39. The SEP for fiber width (1.85-µm) was similar to the results reported by Schimleck and Evans (2004) (SEP=1.7-µm), Schimleck et al. (2004) (SEP=1.7-µm) and Jones et al. (2005) (SEP=1.17-µm). Fiber width shows less radial variation from pith to bark than fiber length (Evans 1994), consequently weaker statistics would be expected. It is possible that a stronger calibration and prediction statistics were acquired for fiber length because of the orientation of the NIR beam to the sample. Owing to our sampling methodology, NIR energy may have had a greater interaction with length, and consequently information relating to fiber length may be reflected in the spectra to a greater extent than that for fiber width (Evans 1994, Schimleck and Evans 2004, Jones et al. 2005).

Gindl et al. (2001) suggested that an indirect influence of cellulose microfibrils may be present in NIR models, because of the chemical composition of the surface of a cell wall. Cellulose microfibrils are small in diameter, but very long, so more cellulose is exposed to NIR when fiber length is measured. The crystallinity of cellulose may be an additional factor which has been proposed to exert an influence on modeled fiber properties.

Relationships between wood properties

The correlations between specific gravity, fiber length, and fiber width are shown in Table 5. Linear models were developed between these three properties. Specific gravity explained 27% of the variation in fiber length (B_0=380.7-µm, B_1=3927.1-µm) (Figure 6).

Specific gravity explained 32% of the variation in fiber width (B_0=34.09-µm, B_1=12.11-µm) (Figure 7). Fiber width explained 52% of the variation in fiber length (B_0=-4662.5-µm, B_1=170.99-µm) (Figure 8). The relationship between SG and fiber length was poor which we attribute to differences in specific gravity with tree heights; fiber length tends to increase with height at similar cambial ages. Splitting the data into different heights, with disks taken below 1-m, between 1 to 3.1-m, and above 3.1-m, showed large improvements in the models. With samples collected from disks below 1-m, the specific gravity explained 51% of the variation in fiber length (B_0=-578.5-µm, B1=5065.2-µm) (Figure 9). With samples collected from disks from 1 to 3.1-m, the specific gravity explained 45% of the variation in fiber length (B_0=-344.7-µm, B_1=5440.8-µm) (Figure 10). With samples collected from disks above 3.1-m, the specific gravity explained 32% of the variation in fiber length (B_0=308.5-µm, B_1=4601.6-µm) (Figure 11).

Table 5. Correlation between wood properties

Property	Fiber width	Specific gravity
Fiber length	0.7413	0.5227
Fiber width		0.3859

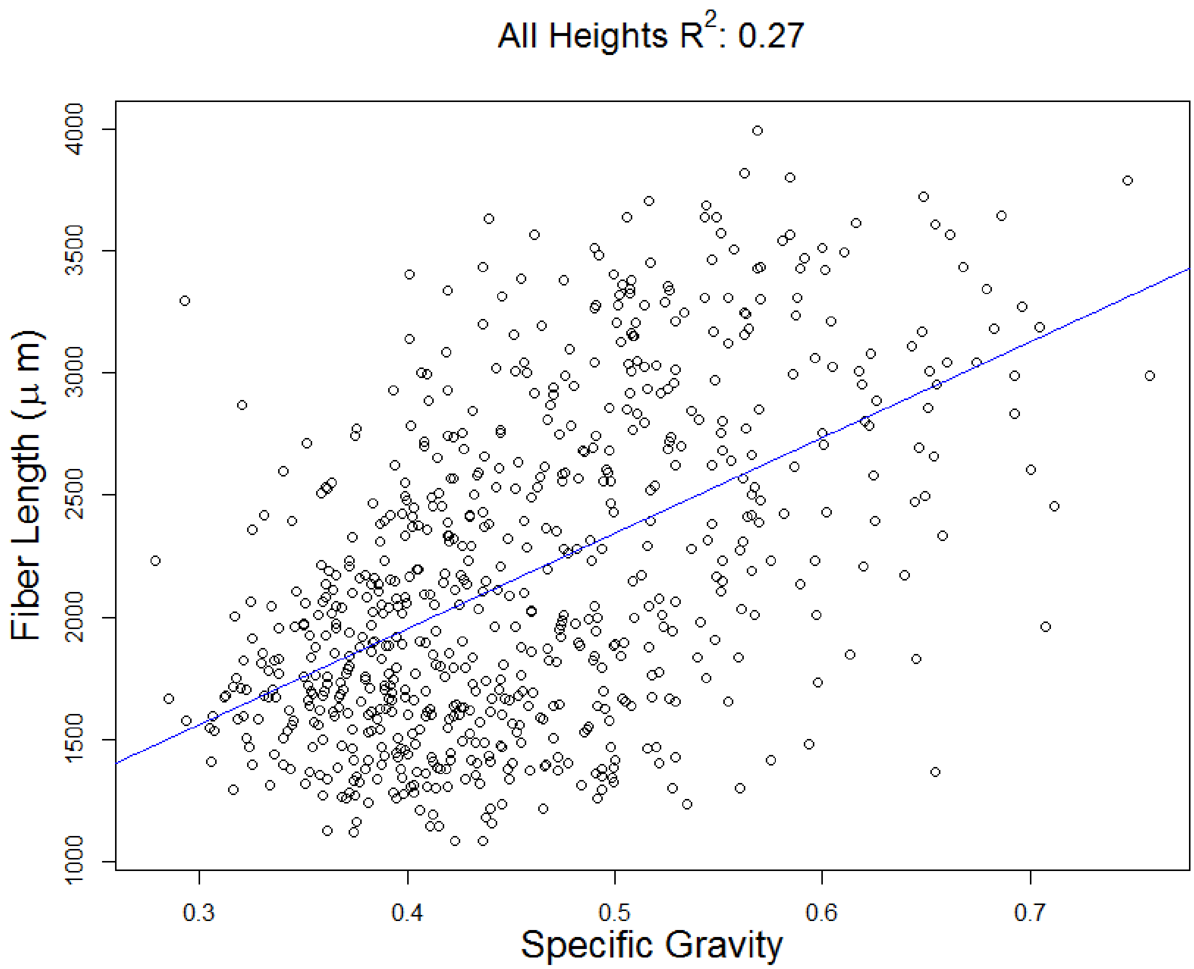

Figure 6. The relationship between fiber length (μm) and specific gravity for all samples

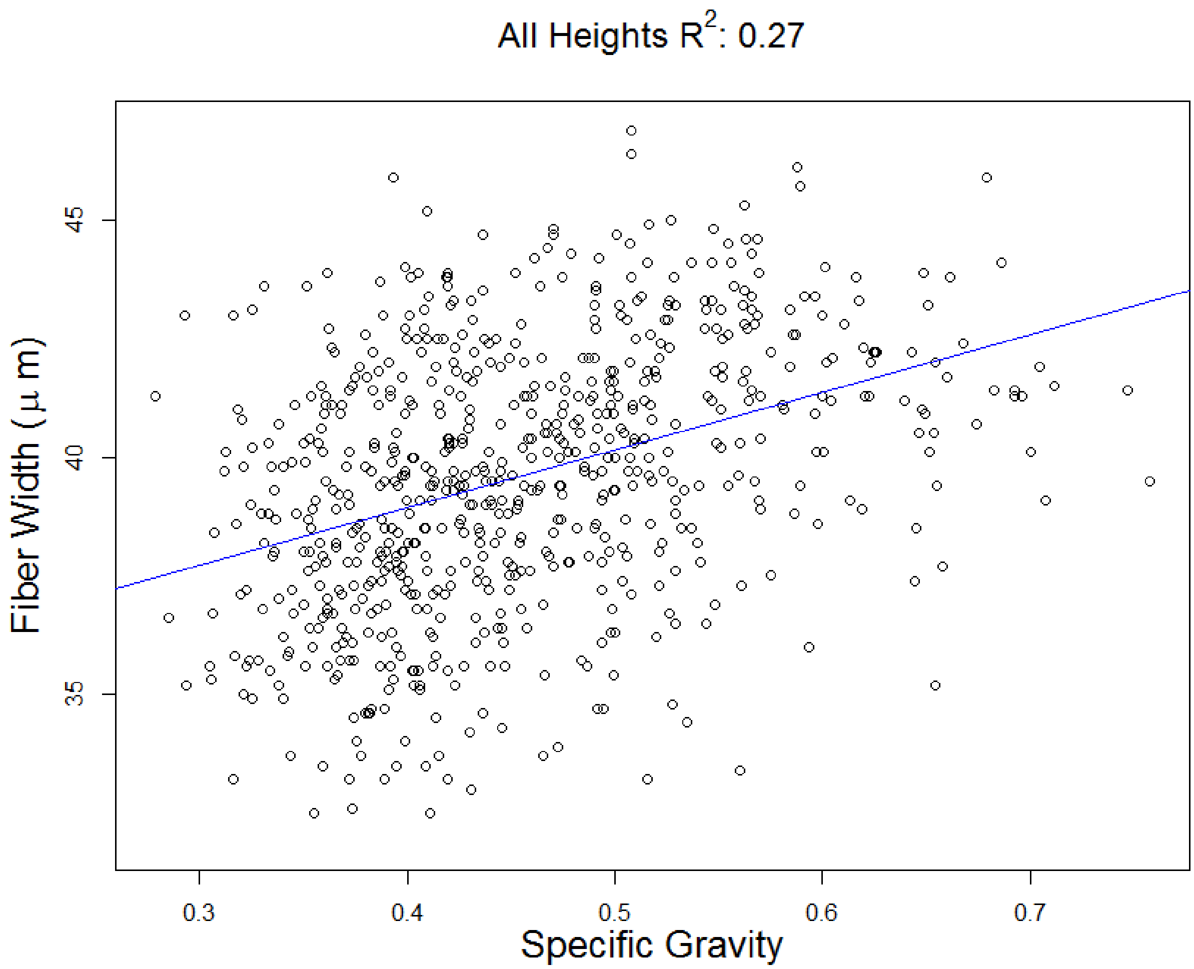

Figure 7. The relationship between fiber width (µm) and specific gravity for all samples

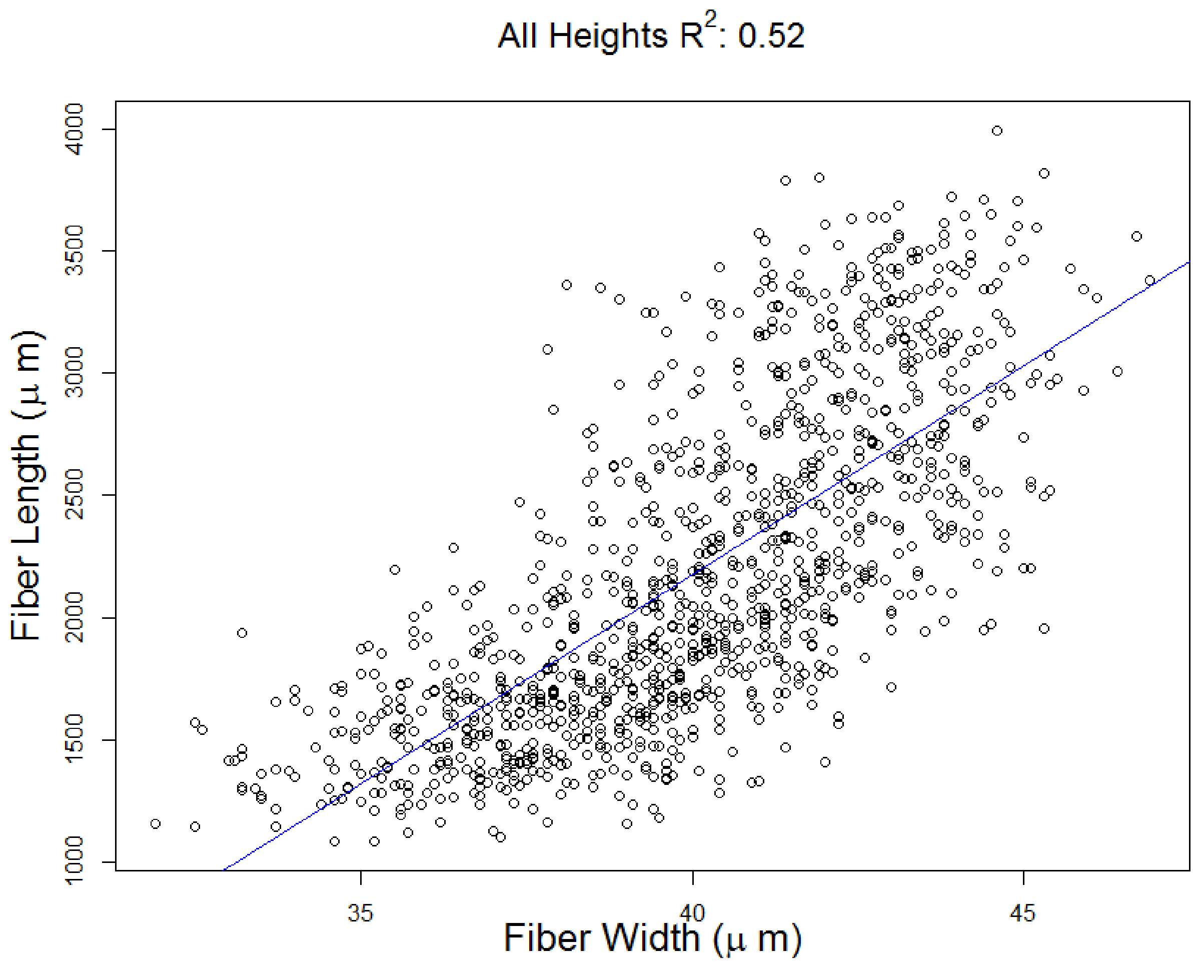

Figure 8. The relationship between fiber length (µm) and fiber width (µm) for all samples

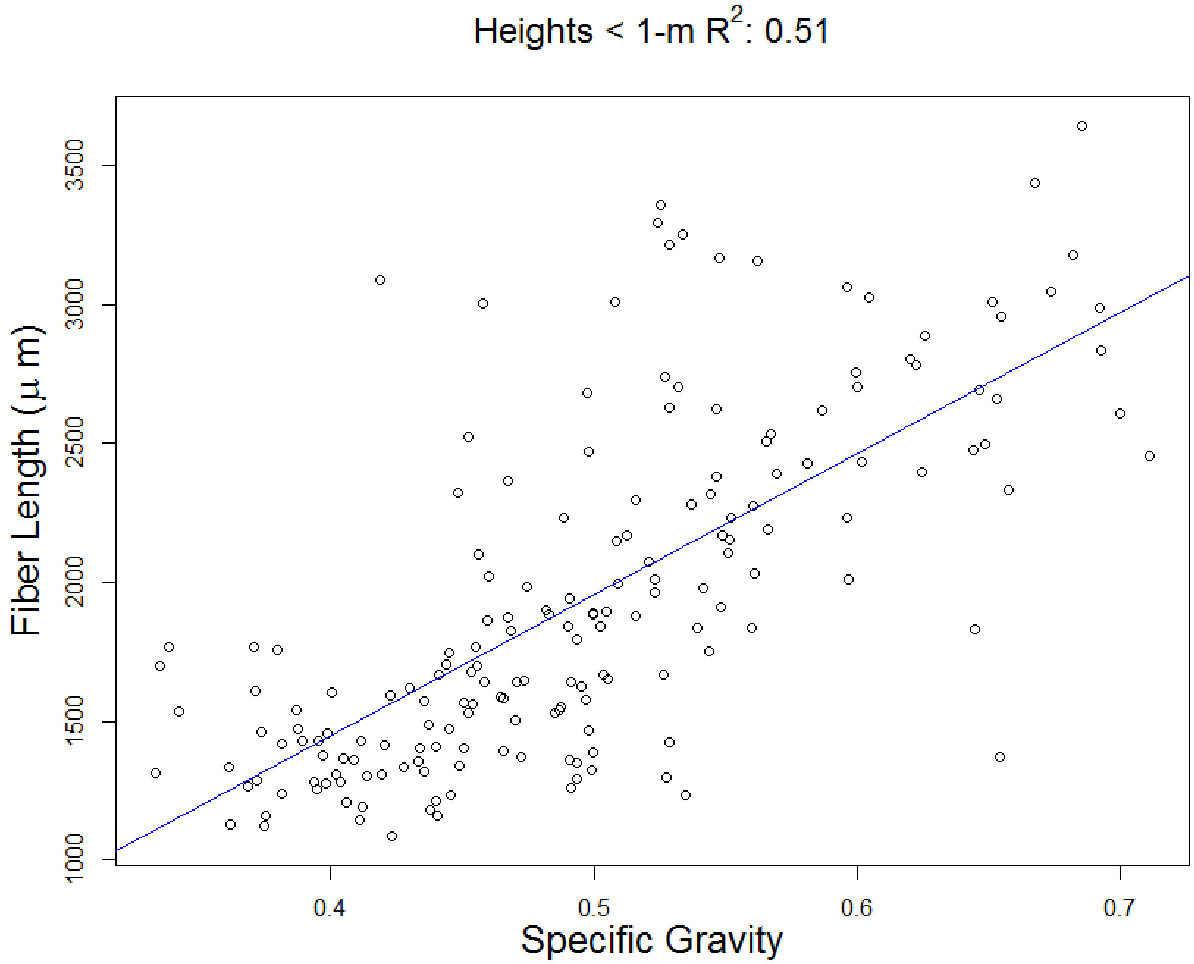

Figure 9. The relationship between fiber length (µm) and specific gravity for samples below 1-m

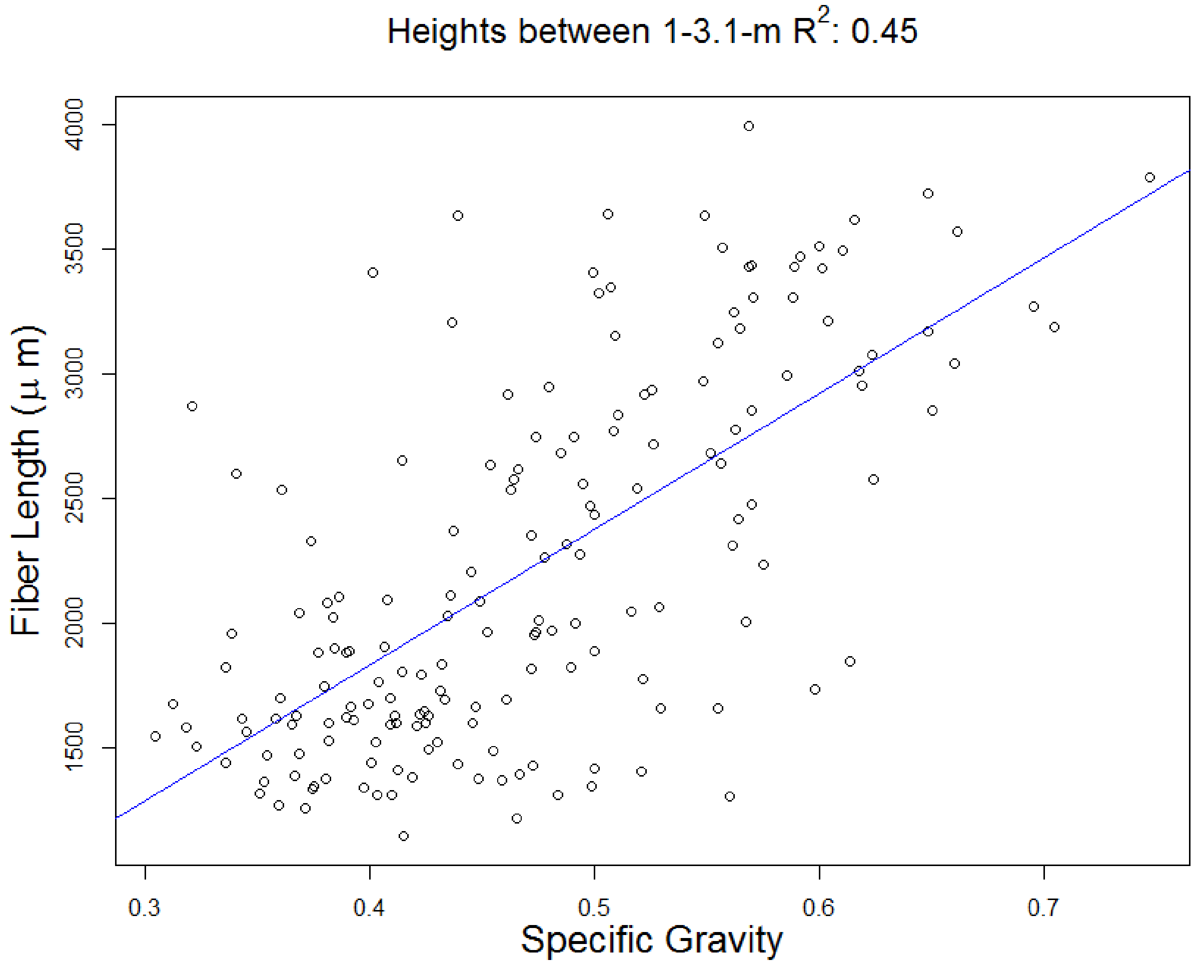

Figure 10. The relationship between fiber length (μm) and specific gravity for samples between 1-3.1-m

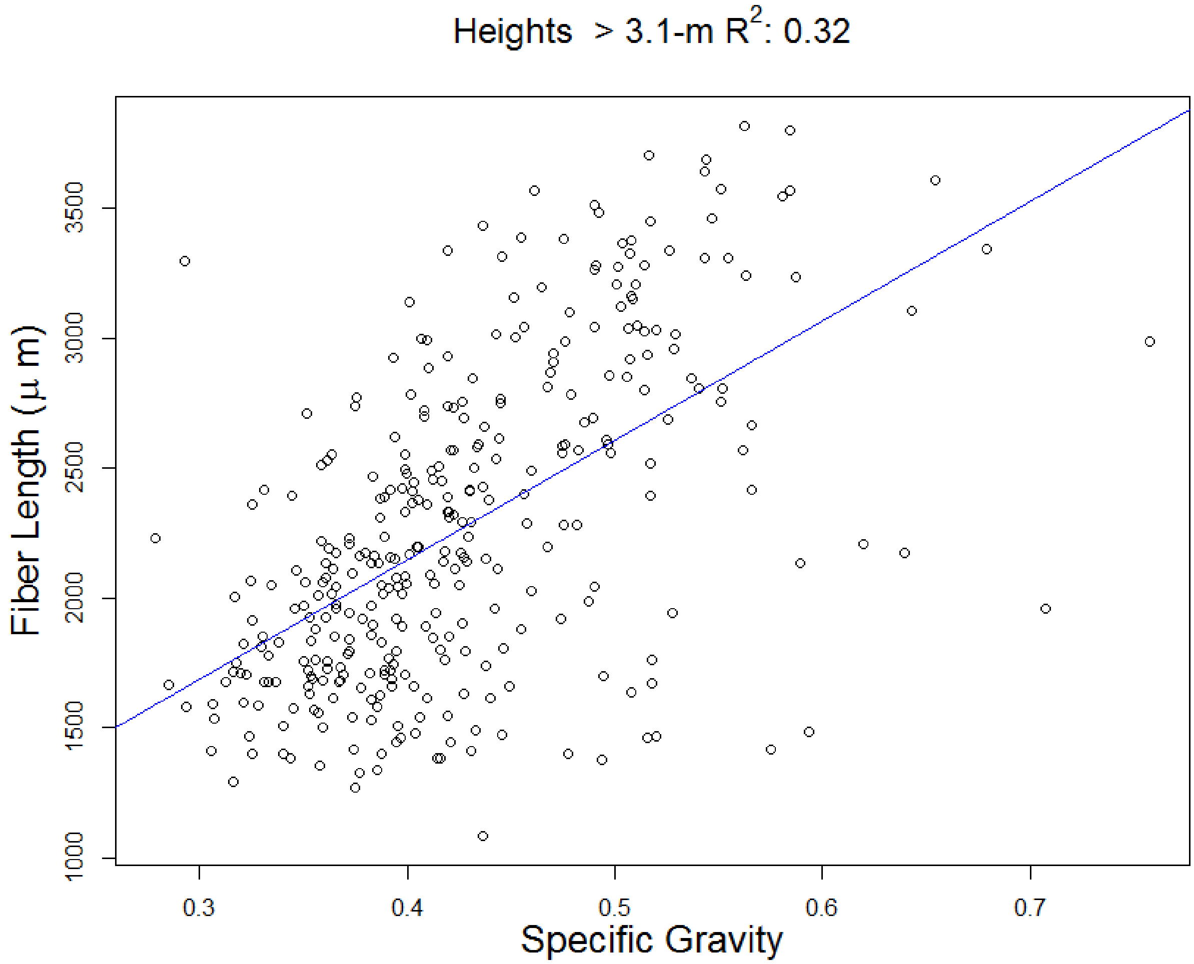

Figure 11. The relationship between fiber length (μm) and specific gravity for samples above 3.1-m

The relationship between fiber length and fiber width for all samples is presented in Figure 8. While fiber length increases, fiber width increases accordingly, and there is a moderate coefficient of determination between the two (R^2=0.52). When samples were segregated by height, the relationship between fiber length and fiber width did not increase significantly.

Regardless of height, specific gravity is low near the pith and increase outwards, providing an inner core of low-density material (Megraw 1985). This variation within the tree is physiological in origin. Final cell size and the rate of cell division are both influenced by growth regulators. Cell wall thickness is related to both the speed of wall deposition and the time duration over which it takes place. The length of the accrual period is thought to be more important of the two, and to also be auxin-controlled. Seasonal onset of latewood formation (smaller cells, thicker walls) seems to coincide with cessation of height growth by the terminal shoot. These phenomena influence cell formation (Megraw 1985, Hemsley and Poole 2004, Stokke and Groom 2008). The specific gravity of an individual cell is largely related to its distance down the trunk from the active crown and to the time of its formation within the season (Megraw 1985, Williams and Megraw 1994).

Within-tree variation in fiber length and fiber width

Fiber length increases from pith to bark (Figure 12). We found differences in fiber length from pith to bark as a function of ring number and height (Figure 13). The cross-sectional pattern for loblolly pine fiber length with age from the pith, segregated by heights, is shown in Figure 13. Regardless of heights, fiber length is shortest near the pith. Fiber length in samples below 1-m range from 1300-µm near the pith and increases with cambial age to about 3000-µm in ring 25. The overall trend for samples between 1 to 3.1-m is the same as samples below 1-m, but fiber length in samples between 1 to 3.1-m increases at a faster rate especially in the first 10 rings from the pith (from 1500-µm at ring 2 to 2700-µm at ring 10) and after the 10^{th} ring slows down considerably between ages 10 and 20 (reaches to 3300-µm at ring 20 from the pith). Fiber length in the samples above 3.1-m increases at a very fast pace within first three rings from the pith (from 1700-µm to 2200-µm) and after first three rings increase with a stable rate and reach 3500-µm at ring 20 from the pith. These results show that fiber length increases from pith to bark, and longitudinally as well. This rate increases slowest at the base, rapidly increases in rate up to 1 to

3.1-m in height, and then becomes approximately stable for heights above that point. The rate which fiber length increases in the vertical axis is different and varies with tree height and cambial age. While the trend explained above applies to all heights, the increase in fiber length with age outward from the pith takes place at a slower rate near the base of the tree than it does at upper heights (lower height=2000-µm, mid-height=2700-µm, top height=3000-µm). For a given number of rings from the pith, average fiber length will be shorter at the base of the stem and breast height region than at heights of several meters and above. We did not see the fiber length reach an asymptote in any of the heights. In this study, we used samples with ages between 19-31 years. Thus it would be useful to include samples from older trees (more than 31 years old) to better understand if the fiber length keeps on increasing with age in any of the heights.

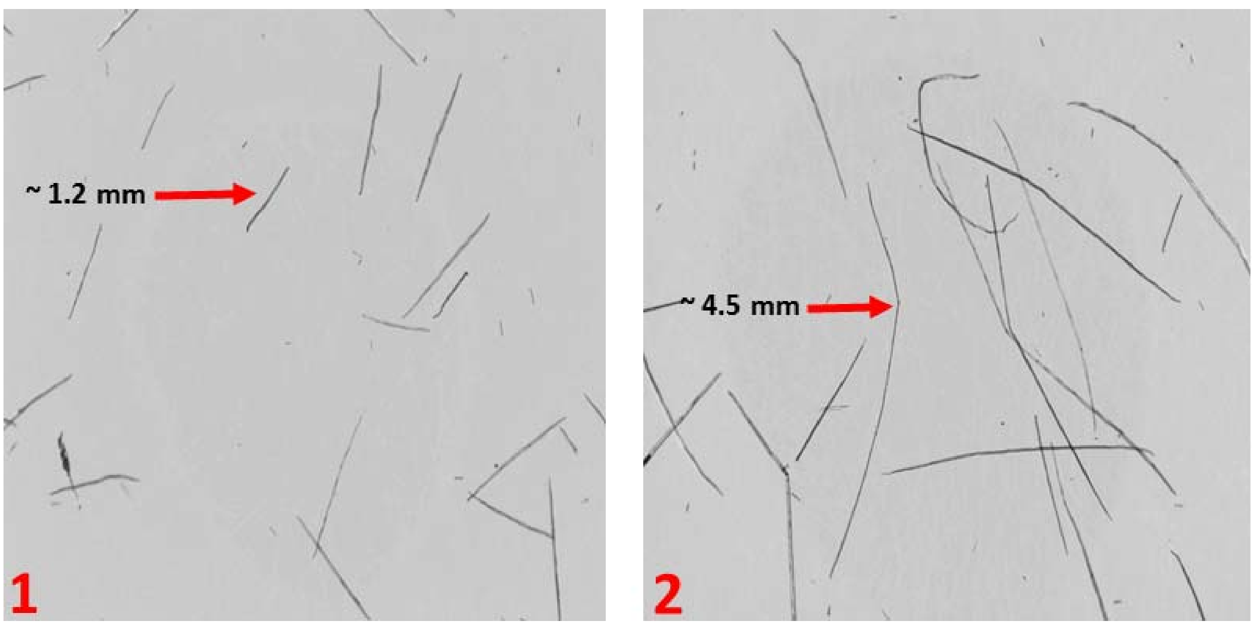

Figure 12. Fiber length varies radially outward from pith with age. (1) fibers at the pith, (2) fibers near the bark

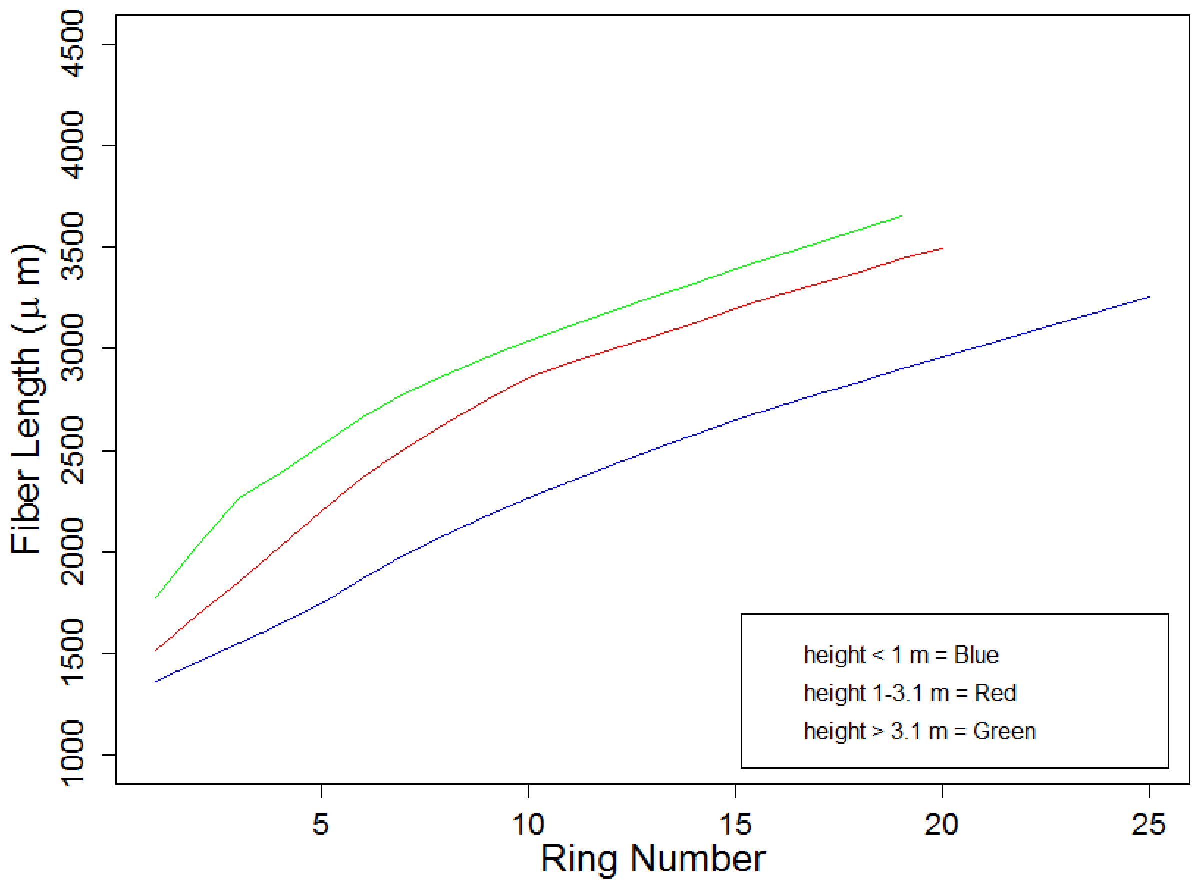

Figure 13. The relationship between fiber length (µm) and ring number, by height within-tree. Blue line shows samples below 1-m, red line shows samples between 1-3.1-m and green show sample above 3.1-m

Fiber length increases with distance from the pith (Figure 14). Fiber length in samples below 1-m increases with a fast rate within the first 8-cm from the pith (from 1300-µm to 2100-µm), and after 10-cm, increases at a slower rate to 2600-µm at 15-cm from the pith. Fiber length of samples between 1 to 3.1-m increases at a fast rate from 1500-µm to 2800-µm in first 7-cm from the pith, and then continues to increases at a slower rate to 13-cm from the pith (3200-µm). The rate of which fiber length increases in samples above 3.1-m is fast in the first 5-cm from the pith (from 1700-µm and to 2700-µm) and increases at a slower rate, later on, and reaches 3500-µm at 13-cm from the pith.

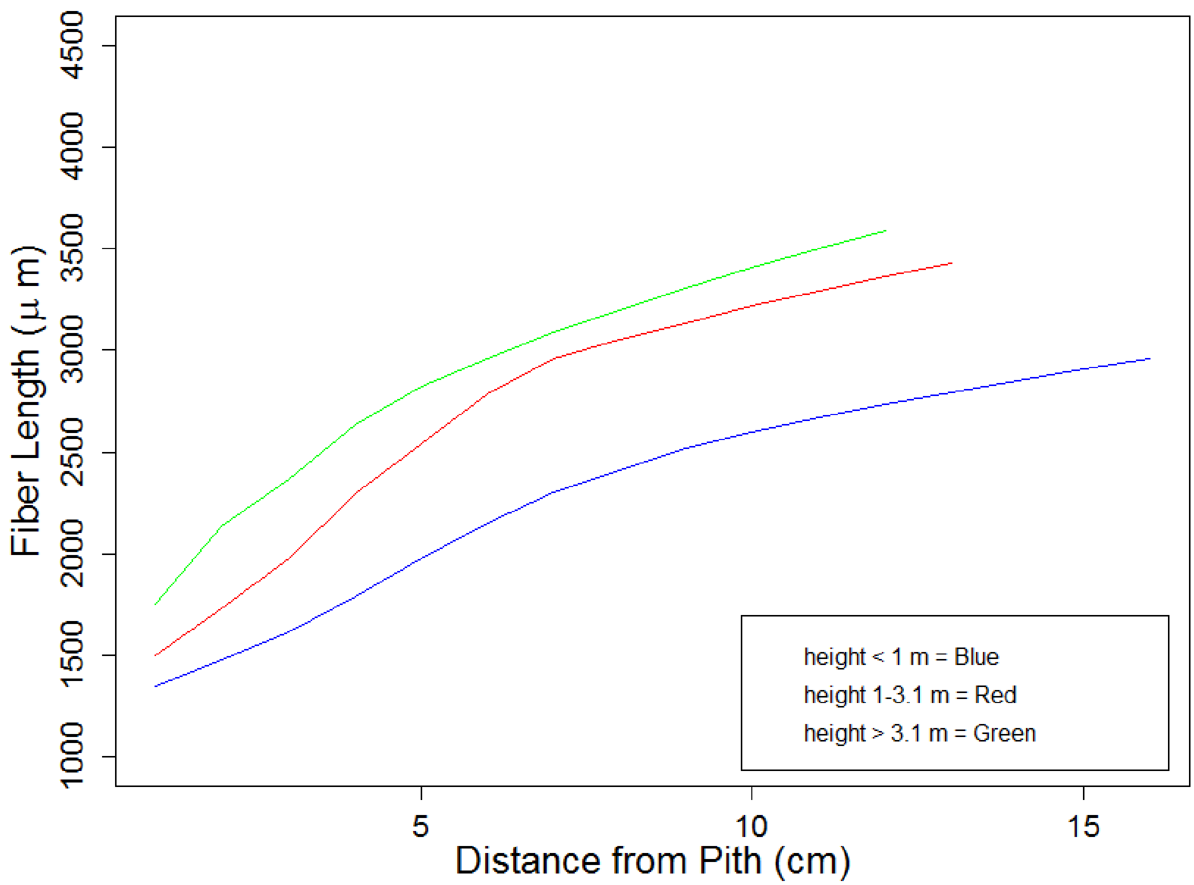

Figure 14. The relationship between fiber length (µm) and distance from the pith (cm), by height within-tree. Blue line shows samples below 1-m, red line shows samples between 1-3.1-m and green show sample above 3.1-m

Fiber width followed a similar trend as fiber length increasing with increasing sampling height and distance from the pith (Figure 15, Figure 16). Fiber width is shortest next to the pith (lower height=36-µm, mid-height=37.5-µm, top height=37.3-µm). The increase outward with age is very fast from rings 1 to 5 (lower hieght=39.2-µm, mid-height=40.8-µm, top height=42-

μm), considerably slower between ages 10 and 20, and very gradually after age 20. Similar to fiber length, fiber width did not reach an asymptote. Older trees should be sampled in the future to gain a better understanding of fiber width patterns.

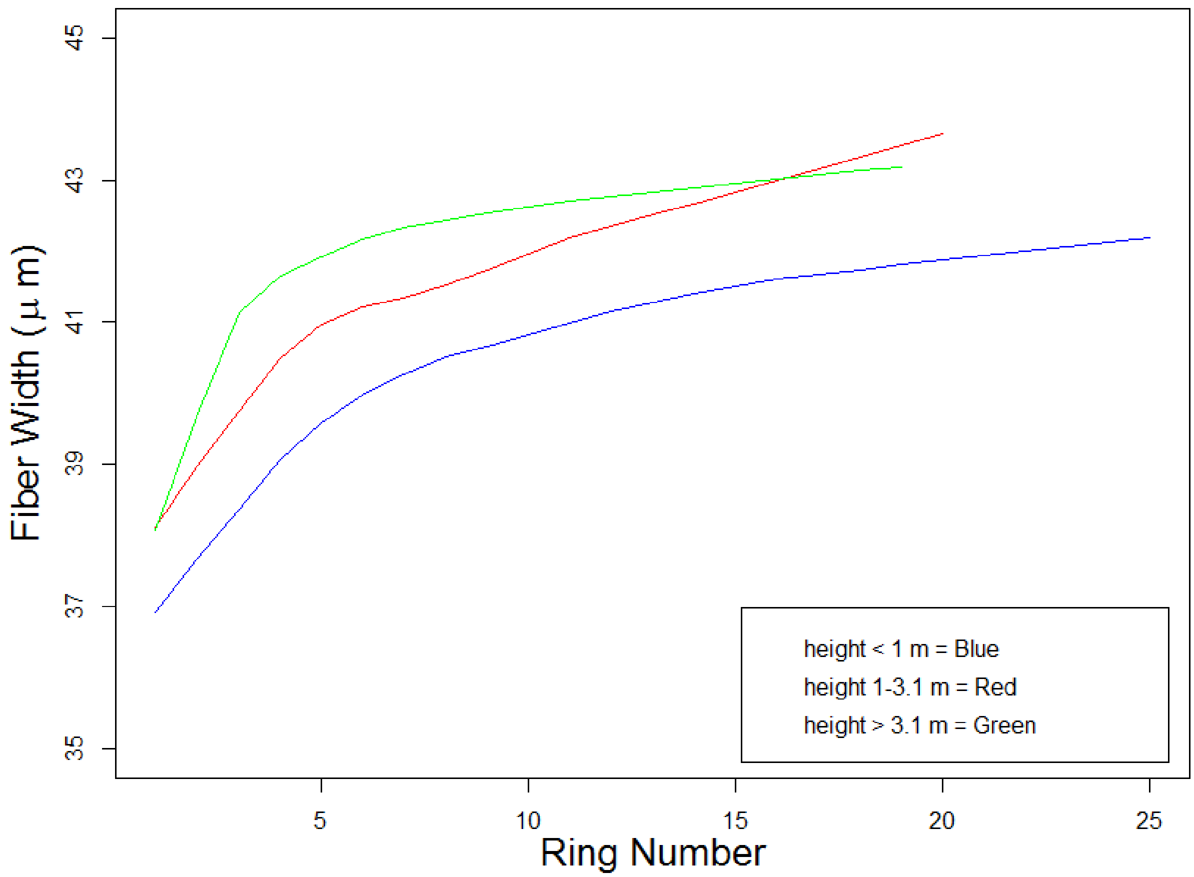

Figure 15. The relationship between fiber width (μm) and ring number, by height within-tree. Blue line shows samples below 1-m, red line shows samples between 1-3.1-m and green show samples above 3.1-m

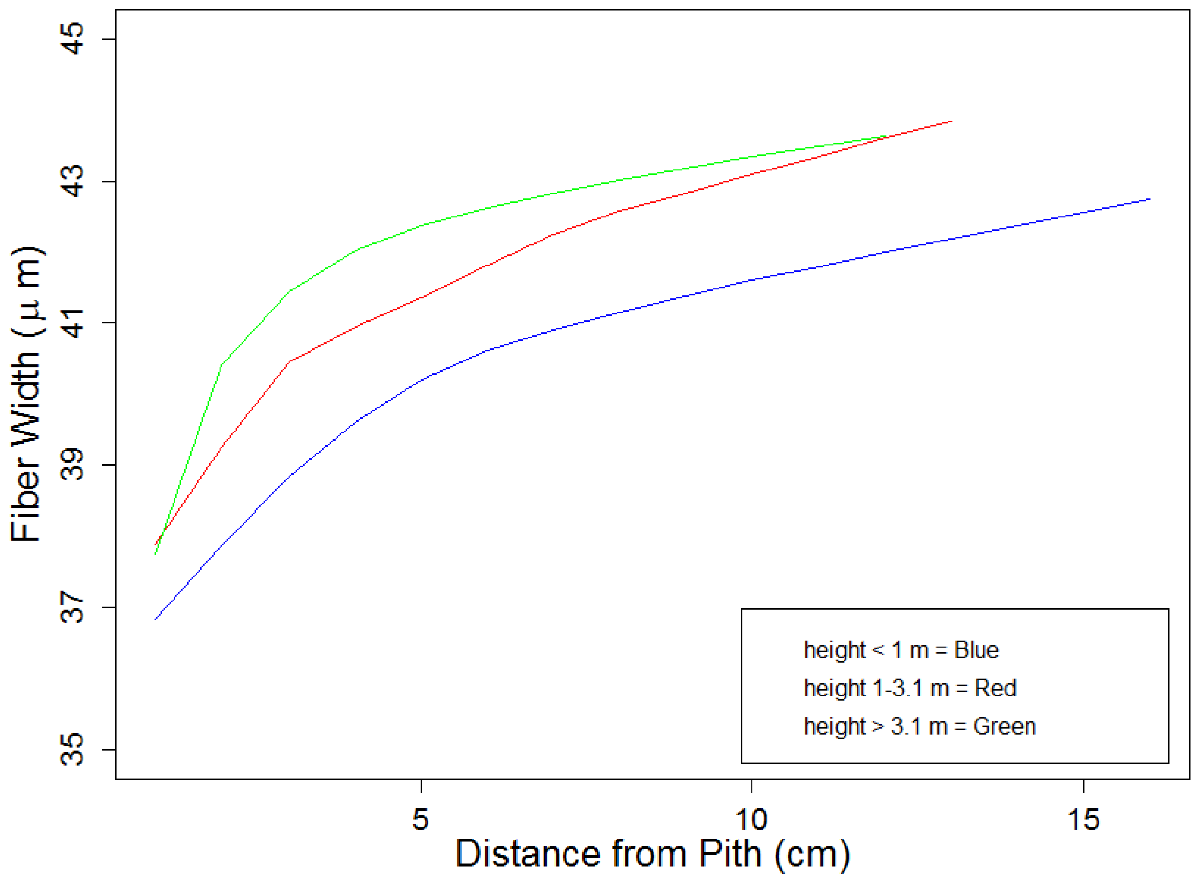

Figure 16. The relationship between fiber width (μm) and distance from the pith (cm), by height within-tree. Blue line shows samples below 1-m, red line shows samples between 1-3.1-m and green show samples above 3.1-m

Antony et al. (2010) observed that in loblolly pine SG decreased in a nonlinear fashion with tree height and concluded that the stem could be divided into three zones based on the longitudinal variation of specific gravity. The height trend they found was that SG decreases rapidly from the base of the tree to heights of 1-m, specific gravity then decreases at a decreasing rate between the height of 1-m to 3.1-m. For heights more than 3.1-m, specific gravity decreases at a constant rate. For fiber length, we found opposite trend where fiber length increases within those three height zones, then stabilizes. The three segmented classification of loblolly pine height level as proposed by Burdon et al. (2004) and Antony et al. (2010) work well for explaining fiber length variation.

Specific gravity increases from the pith to bark at all heights, with the highest values near the bark at the base of the tree (Megraw 1985). In 20 to 25 years old trees, at the base of the stem SG is high (0.55) and decreases very rapidly to relative height of 0.1 (0.46), decreases at a descending rate from a relative height of 0.1 to 0.3 (from 0.46 to 0.43), and then decreases at a constant rate above a relative height 0.3 to the top of the tree (0.35) (Antony et al. 2010). The results of this study depicted that fiber length does not follow longitudinal specific gravity variation but has the same radial variation from pith to bark. Fiber length is low at the base of the stem and increases with height, and it has the highest values in rings close to the bark.

Microfibril angle varies from pith to bark, with the highest angles occurring in the first five growth rings from the pith at the base of the tree (Xu et al. 2004). At the base of the stem MFA is high (35°) and decreases to 27° with height 3.1-m, and decreases to 12° with height 10-m (Jordan et al. 2007). In conifers, the MFA becomes stable at approximately ring 20 at breast height and ring ten at 8-m height (Donaldson 2008). The result of our study demonstrated that fiber length follows MFA in terms of within-tree variation but in reverse order (Jordan et al. 2006). Unlike MFA, fiber length has the highest values in rings close to the bark. Fiber length is low at the base of the stem and increases with height. Fiber length is short near the pith and increases outward with age. An average fiber length from the first ten or so rings from the pith can be expected to be considerably lower (1300-μm) than that of material taken farther away from the pith (3000-μm). This variation is true regardless of height, but the rate of change is different based on sample height.

The knowledge of the specific gravity and fiber length distribution within a tree is necessary to decide at which height samples should be taken to represent the whole tree. Past investigations were performed to find a representative sampling height for specific gravity (Trincado et al. 2007, Antony et al. 2012, Deng et al. 2014). As an optimal sampling height for fiber length in *P. taeda* is still unknown, but the initial results suggest that large changes occur in first log (< 5-m in height) and thus future studies should emphasize sampling this region more intensively than this study which sampled every 1.5-m in height.

Logistic regression model for fiber length and fiber width

The relationship between fiber length and ring number using 3-parameter logistic regression for fiber length is presented in Figure 17. The 3-parameter logistic regression equation is:

$$(2)\ DV = \frac{\text{Asym}}{1+e^{\left(\frac{xmid-ring}{scale}\right)}}$$

Where the *DV* is dependent variable (fiber length or fiber with), *Asym* is a numeric parameter representing the asymptote, *xmid* is value at the inflection point of the logistic curve, *scal* is a scaling parameter for the x-axis, and *ring* is the cambial age effect. The model predictions follow the observed fiber length trend; fiber length increases from pith to bark and this increase happens regardless of height. The rate of increase in upper part of tree is faster than increase rate in lower part of the stem. The relationship between fiber width and ring number usisng 3-parameter logistic regression for fiber width is showed in Figure 18. Regardless of height, fiber width increases from pith to bark, but the rate of increase in lower part of the stem is lower than the rate at upper section of the tree. The model coefficients and root mean square error (RMSE) for fiber length and fiber width are summarized in Table 6.

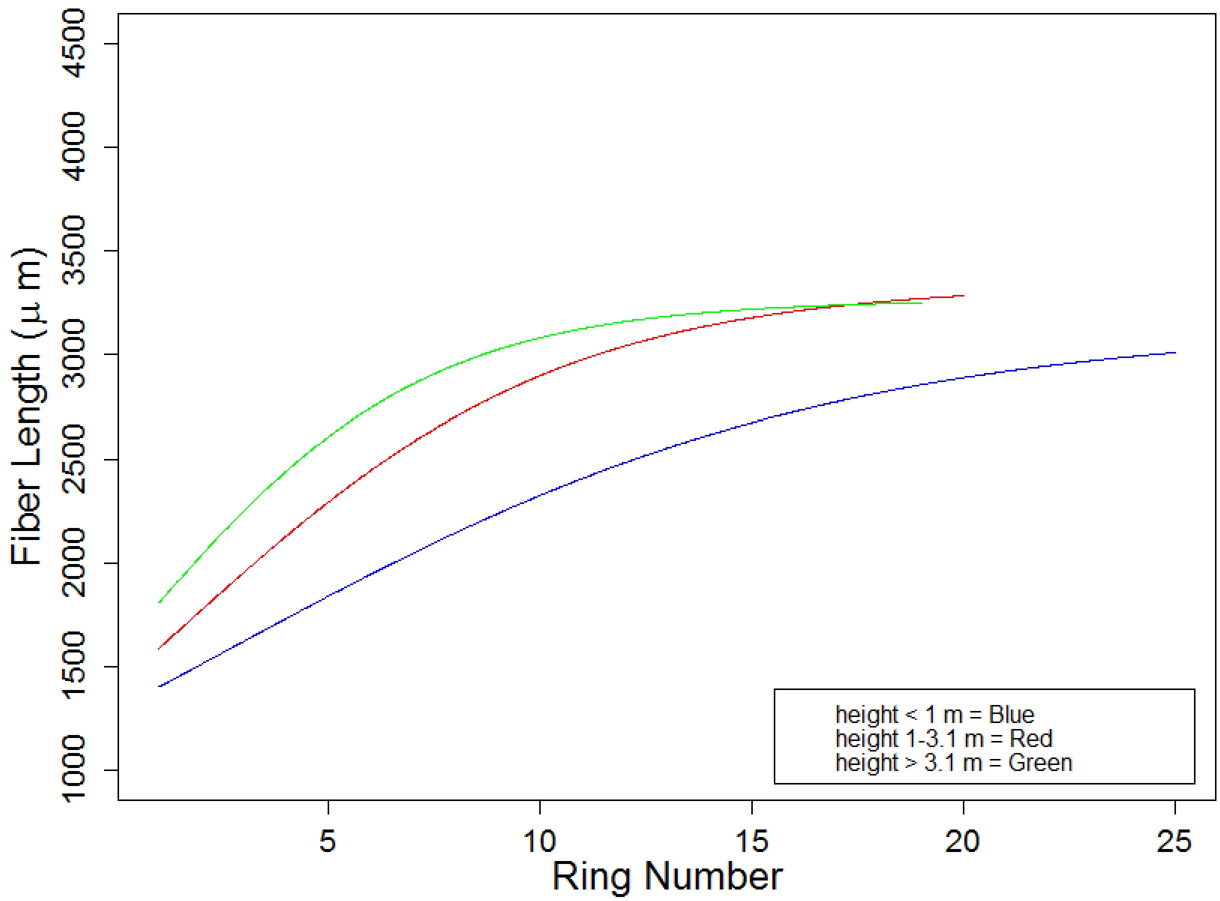

Figure 17. The relationship between predicted fiber length (µm) and ring number, by height within-tree. Lines represent mean trend using 3-parameter logistic regression model

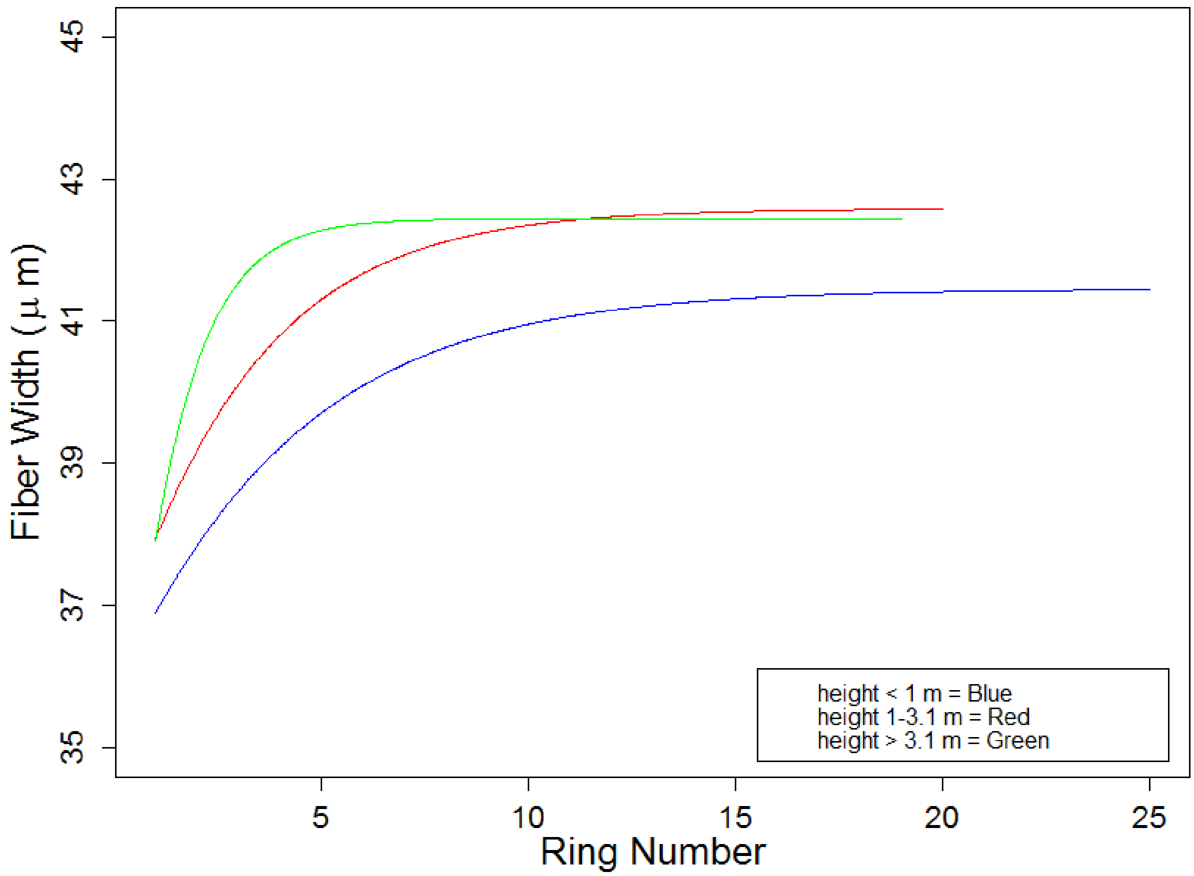

Figure 18. The relationship between predicted fiber width (µm) and ring number, by height within-tree. Lines represent mean trend using 3-parameter logistic regression model

Table 6. The model coefficients and root mean square error for fiber length (μm) and fiber width (μm)

Property	Height	Asym	xmid	scal	RMSE
Fiber length (μm)	stump to top	3156.35	0.28	4.88	448.36
	< 1 m	3138.25	2.51	7.13	369.55
	1-3.1-m	3338.46	1.43	4.54	406.01
	> 3.1-m	3263.37	0.25	3.44	338.28
Fiber width (μm)	stump to top	41.91	-2.97	1.80	2.12
	< 1 m	41.44	-7.09	3.86	1.91
	1-3.1-m	42.58	-5.12	2.91	1.93
	> 3.1-m	42.43	-1.47	1.16	2.01

CHAPTER 5

CONCLUSION

The purpose of this study was to examine the within-tree variation of loblolly pine fiber properties. We scanned 1,842 samples from pith to bark using NIR spectroscopy to develop calibrations for fiber properties. Based on the RPD_p and R_p^2 values obtained from PLS regression models; there was a strong correlation between fiber length measurements and the NIR estimates (R_p^2=0.84, SEP=261.5-μm ,RPD_p=2.5). These results demonstrate that NIR spectroscopy has the potential to predict fiber length of *P. taeda* with relatively high accuracy, and fulfill the requirements of AACC Method 39-00 for screening in breeding programs ($RPD \geq 2.5$). Unlike fiber length, the RPD_p (1.39) and R_p^2(0.49) values obtained for fiber width had moderate relationships. In the future, we can predict tracheid length on the 1,842 samples using the model we developed here.

Within-tree variation of fiber length and width showed opposite pattern reported for MFA. Unlike MFA, fiber length has the highest value in rings close to the bark. Fiber length is low at the base of the stem and increases with height in the lower stem, but decreases near the top of the stem. Fiber length is short near the pith and increases outward with age, an average fiber length of material from the first ten rings from the pith can be expected to be considerably lower than that of material taken farther away from the pith. This is true regardless of height. The increase in length with age from the pith occurs at a faster rate at greater heights than near the base of the stem. The variation in wood characteristics within a tree is widely associated with a radial and vertical position within the stem (Megraw 1985, Donaldson 2008).

Although this is likely the largest fiber length study done on loblolly pine, we feel that it would be useful to sample trees older than 31 years to better understand if the fiber length continues increasing with age in the segmented heights because we did not see fiber length reaching an asymptote with this data. Further investigations including a greater number of older trees will reveal where the asymptotes occur.

REFERENCES

AACC. 1999 AACC method 39-00.01. Near-infrared methods—guidelines for model development and maintenance. St. Paul, MN, U.S.A.

Alves, A., Santos, A., Silva Perez, D., Rodrigues, J., Pereira, H., Simões, R. *et al.* 2007 NIR PLSR model selection for Kappa number prediction of maritime pine Kraft pulps. *Wood Science and Technology*, **41** (6), 491-499.

Antony, F. 2010 *Modeling the Wood Properties of Loblolly Pine (Pinus taeda L.) Growing in Southern United States.* Doctorate of Philosophy, University of Georgia.

Antony, F., Jordan, L., Schimleck, L.R., Clark, A., Souter, R.A. and Daniels, R.F. 2011 Regional variation in wood modulus of elasticity (stiffness) and modulus of rupture (strength) of planted loblolly pine in the United States. *Canadian Journal of Forest Research*, **41** (7), 1522-1533.

Antony, F., Schimleck, L.R. and Daniels, R.F. 2012 Identification of representative sampling heights for specific gravity and moisture content in plantation-grown loblolly pine (Pinus taeda). *Canadian Journal of Forest Research*, **42** (3), 574-584.

Antony, F., Schimleck, L.R., Daniels, R.F., Clark, A. and Hall, D.B. 2010 Modeling the longitudinal variation in wood specific gravity of planted loblolly pine (Pinus taeda) in the United States. *Canadian Journal of Forest Research*, **40** (12), 2439-2451.

Antony, F., Schimleck, L.R., Jordan, L., Hornsby, B., Dahlen, J., Daniels, R.F. *et al.* 2013 Growth and wood properties of genetically improved loblolly pine: propagation type comparison and genetic parameters. *Canadian Journal of Forest Research*, **44** (3), 263-272.

ASTM-D2395. 2014 Standard Test Methods for Density and Specific Gravity (Relative Density) of Wood and Wood-Based Materials. *ASTM D-2395, United States*.

Auty, D., Gardiner, B.A., Achim, A., Moore, J.R. and Cameron, A.D. 2013 Models for predicting microfibril angle variation in Scots pine. *Annals of Forest Science*, **70** (2), 209-218.

Bailey, I.W. 1958 The structure of tracheids in relation to the movement of liquids, suspensions, and undissolved gases. *Thimann, KV The physiology of forest trees. Ronald Press Co: New York*, 71-82.

Baldwin, V.C., Peterson, K.D., Clark, A., Ferguson, R.B., Strub, M.R. and Bower, D.R. 2000 The effects of spacing and thinning on stand and tree characteristics of 38-year-old loblolly pine. *Forest Ecology and Management*, **137** (1), 91-102.

Borch, J., Lyne, M.B., Mark, R.E. and Habeger, C.C. 2001 *Handbook of Physical Testing of Paper*. CRC Press.

Borders, B.E. and Bailey, R.L. 2001 Loblolly Pine - Pushing the Limits of Growth. *Southern Journal of Applied Forestry*, **25** (2), 69-74.

Briggs, D.G. and Smith, W.R. 1986 Effects of Silvicultural Practices on Wood Properties of Conifers: A Review. *Douglas fir: stand management for the future. University of Washington Press, Seattle, WA*, 108-117.

Burdon, R.D., Kibblewhite, R.P., Walker, J.C., Megraw, R.A., Evans, R. and Cown, D.J. 2004 Juvenile Versus Mature Wood: A New Concept, Orthogonal to Corewood Versus Outerwood, with Special Reference to Pinus radiata and P. taeda. *Forest science*, **50** (4), 399-415.

Burns, D.A. and Ciurczak, E.W. 2007 *Handbook of Near-Infrared Analysis*. 3rd edn. CRC Press, 808 p.

Carvalho, M.G., Ferreira, P.J., Martins, A.A. and Figueiredo, M.M. 1997 A comparative study of two automated techniques for measuring fiber length.

Chung, H., Choi, S.-Y., Choo, J. and Lee, Y. 2004 Investigation of partial least squares (PLS) calibration performance based on different resolutions of near infrared spectra. *Bulletin-Korean Chemical Society*, **25** (5), 647-651.

Clark, A., Jordan, L., Schimleck, L. and Daneils, R.F. 2008 Effect of initial planting spacing on wood properties of unthinned loblolly pine at age 21. *Forest Product Journal*, **58** (10), 78-83.

Courchene, C.E., Peter, G.F. and Litvay, J. 2006 Cellulose Microfibril Angle as a Determinant of Paper Strength and Hygroexpansivity in Pinus taeda L. *Wood and Fiber Science*, **38** (1), 112-120.

Cramer, S., Kretschmann, D., Lakes, R. and Schmidt, T. 2005 Earlywood and latewood elastic properties in loblolly pine. *Holzforschung*, **59** (5), 531-538.

Craven, P. and Wahba, G. 1978 Smoothing Noisy Data with Spline Functions. *Numerische Mathematik*, **31** (4), 377-403.

Dahlen, J., Diaz, I., Schimleck, L. and Jones, P.D. 2016 Near-infrared spectroscopy prediction of southern pine No. 2 lumber physical and mechanical properties. *Wood Science and Technology*, 1-14.

Deng, X., Zhang, L., Lei, P., Xiang, W. and Yan, W. 2014 Variations of wood basic density with tree age and social classes in the axial direction within Pinus massoniana stems in Southern China. *Annals of Forest Science*, **71** (4), 505-516.

Donaldson, L. 2008 Microfibril angle: Measurement, variation and relationships - A review. *IAWA Journal*, **29** (4), 345.

Evans, R. 1994 Rapid Measurement of the Transverse Dimensions of Tracheids in Radial Wood Sections from Pinus radiata. *Holzforschung-International Journal of the Biology, Chemistry, Physics and Technology of Wood*, **48** (2), 168-172.

Filzmoser, P. and Varmuza, K. 2016 Multivariate Statistical Analysis in Chemometrics.

Franklin, G. 1945 Preparation of thin sections of synthetic resins and wood-resin composites, and a new macerating method for wood. *Nature*, **155** (3924), 51.

Fujimoto, T., Kurata, Y., Matsumoto, K. and Tsuchikawa, S. 2008 Application of near infrared spectroscopy for estimating wood mechanical properties of small clear and full length lumber specimens. *Journal of Near Infrared Spectroscopy*, **16** (6), 529-537.

Gaby, L.I. 1985 The Southern Pines. Forest Service, US Dept. of Agriculture, p. 11.

Gartner, B.L. 2008 Prediction of Wood Structural Patterns in Trees by Using Ecological. In *Characterization of the Cellulosic Cell Wall*, pp. 38.

Gindl, W., Teischinger, A., Schwanninger, M. and Hinterstoisser, B. 2001 The relationship between near infrared spectra of radial wood surfaces and wood mechanical properties. *Journal of Near Infrared Spectroscopy*, **9**, 255.

Granato, D. and Ares, G. 2013 *Mathematical and Statistical Methods in Food Science and Technology*. John Wiley & Sons.

Groom, L., Mott, L. and Shaler, S. 2002 Mechanical properties of individual southern pine fibers. Part I. Determination and variability of stress-strain curves with respect to tree height and juvenility. *Wood and Fiber Science*, **34** (1), 14-27.

Harms, W.R., Whitesell, C.D. and DeBell, D.S. 2000 Growth and development of loblolly pine in a spacing trial planted in Hawaii. *Forest Ecology and Management*, **126** (1), 13-24.

Hauksson, J.B., Bergqvist, G., Bergsten, U., Sjöström, M. and Edlund, U. 2001 Prediction of basic wood properties for Norway spruce. Interpretation of near infrared spectroscopy data using partial least squares regression. *Wood Science and Technology*, **35** (6), 475-485.

Haywood, J.D. 2005 Influence of Precommercial Thinning and Fertilization on Total Stem Volume and Lower Stem Form of Loblolly Pine. *Southern Journal of Applied Forestry*, **29** (4), 215-220.

Hemsley, A.R. and Poole, I. 2004 *The Evolution of Plant Physiology*. Academic Press.

Hoadley, R.B. 1990 *Identifying Wood: Accurate Results with Simple Tools*. Taunton Press.

Hodge, G. and Woodbridge, W. 2004 Use of near infrared spectroscopy to predict lignin content in tropical and sub-tropical pines. *Journal of Near Infrared Spectroscopy*, **12** (6), 381-390.

Höskuldsson, A. 1988 PLS Regression Methods. *Journal of Chemometrics*, **2** (3), 211-228.

Hoyland, R., Howarth, P., Field, R. and Bolam, F. 1976 The Fundamental Properties of Paper Related to its Uses. *Ernest Benn, Tunbridge, Kent*.

Inagaki, T., Schwanninger, M., Kato, R., Kurata, Y., Thanapase, W., Puthson, P. *et al.* 2012 Eucalyptus camaldulensis density and fiber length estimated by near-infrared spectroscopy. *Wood Science and Technology*, **46** (1-3), 143-155.

Ivković, M., Gapare, W.J., Abarquez, A., Ilic, J., Powell, M.B. and Wu, H.X. 2009 Prediction of wood stiffness, strength, and shrinkage in juvenile wood of radiata pine. *Wood science and technology*, **43** (3-4), 237-257.

Jones, D.P. 2006 *Rapid Non-Destructive Estimation of Pinus taeda L. Morphological and Chemical Properties Using Near Infrared*, University of Georgia.

Jones, P.D., Schimleck, L.R., Daniels, R.F., Clark, A. and Purnell, R.C. 2008 Comparison of Pinus taeda L. whole-tree wood property calibrations using diffuse reflectance near infrared spectra obtained using a variety of sampling options. *Wood Science and Technology*, **42** (5), 385-400.

Jones, P.D., Schimleck, L.R., Peter, G.F., Daniels, R.F. and Clark, A. 2005 Non-destructive estimation of Pinus taeda L tracheid morphological characteristics for samples from a wide range of sites in Georgia. *Wood Science and Technology*, **39** (7), 529-545.

Jones, P.D., Schimleck, L.R., Peter, G.F., Daniels, R.F. and Clark, A. 2006 Nondestructive estimation of wood chemical composition of sections of radial wood strips by diffuse reflectance near infrared spectroscopy. *Wood Science and Technology*, **40** (8), 709-720.

Jones, P.D., Schimleck, L.R., Peter, G.F., Daniels, R.F. and Clark Iii, A. 2005 Nondestructive estimation of Pinus taeda L. wood properties for samples from a wide range of sites in Georgia. *Canadian Journal of Forest Research*, **35** (1), 85-92.

Jordan, L., Clark, A., Schimleck, L.R., Hall, D.B. and Daniels, R.F. 2008 Regional variation in wood specific gravity of planted loblolly pine in the United States. *Canadian Journal of Forest Research*, **38** (4), 698-710.

Jordan, L., He, R., Hall, D.B., Clark, A. and Daniels, R.F. 2007 Variation in Loblolly Pine Ring Microfibril Angle in the Southeastern United States. *Wood and Fiber Science*, **39** (2), 352-363.

Jordan, L., Re, R., Hall, D.B., Clark, A. and Daniels, R.F. 2006 Variation in Loblolly Pine Cross-Sectional Microfibril Angle with Tree Height and Physiographic Region. *Wood and Fiber Science*, **38** (3), 390-398.

Kelley, S., Rials, T., Snell, R., Groom, L. and Sluiter, A. 2004 Use of near infrared spectroscopy to measure the chemical and mechanical properties of solid wood. *Wood Science and Technology*, **38** (4).

Kennard, R.W. and Stone, L.A. 1969 Computer Aided Design of Experiments. *Technometrics*, **11** (1), 137-148.

Kibblewhite, R.P. Effects of pulp drying and refining on softwood fibre wall structural organisations, pp. 121-152.

Lachenbruch, B., Johnson, G., Downes, G. and Evans, R. 2010 Relationships of density, microfibril angle, and sound velocity with stiffness and strength in mature wood of Douglas-fir. *Canadian Journal of Forest Research*, **40** (1), 55-64.

Löf, M., Dey, D.C., Navarro, R.M. and Jacobs, D.F. 2012 Mechanical site preparation for forest restoration. *New Forests*, **43** (5), 825-848.

Love-Myers, K.R., Clark, A., Schimleck, L.R., Dougherty, P.M. and Daneils, R.F. 2010 The Effects of Irrigation and Fertilization on Specific Gravity of Loblolly Pine. *Forest Science*, **56** (5), 483-493.

Lundgren, C. 2004 Cell Wall Thickness and Tangential and Radial Cell Diameter of Fertilized and Irrigated Norway spruce. *Silva Fennica*, **38** (1), 95-106.

Lundqvist, S.-O. 2002 Efficient wood and fiber characterization-A key factor in research and operation. *Annals of forest science*, **59** (5-6), 491-501.

Macdonald, E. and Hubert, J. 2002 A review of the effects of silviculture on timber quality of Sitka spruce. *Forestry*, **75** (2), 107-138.

McKenzie, A.W. 1994 *A Guide to Pulp Evaluation*. CSIRO.

Meder, R., Marston, D., Ebdon, N. and Evans, R. 2011 Spatially-resolved radial scanning of tree increment cores for near infrared prediction of microfibril angle and chemical composition. *Journal of Near Infrared Spectroscopy*, **18** (6), 499.

Megraw, R.A. 1985 *Wood Quality Factors in loblolly pine: the influence of tree age, position in tree, and cultural practice on wood specific gravity, fiber length, and fibril angle*. Tappi.

Mevik, B.-H., Wehrens, R. and San Michele all'Adige, T. 2015 Introduction to the pls Package.

Mora, C., Schimleck, L. and Isik, F. 2008 Near infrared calibration models for the estimation of wood density in Pinus taeda using repeated sample measurements. *Journal of Near Infrared Spectroscopy*, **16** (1), 517.

Mora, C.R. 2009 *Rapid Techniques for Screeing Wood Properties in Forest Plantations.* Doctor of Philosophy, University of Georgia.

Mora, C.R. and Schimleck, L.R. 2008 Determination of specific gravity of green Pinus taeda samples by near infrared spectroscopy: comparison of pre-processing methods using multivariate figures of merit. *Wood Science and Technology*, **43** (5-6), 441-456.

Mora, C.R. and Schimleck, L.R. 2008 On the selection of samples for multivariate regression analysis: application to near-infrared (NIR) calibration models for the prediction of pulp yield in Eucalyptus nitens. *Canadian Journal of Forest Research*, **38** (10), 2626-2634.

Mora, C.R. and Schimleck, L.R. 2009 Determination of within-tree variation of Pinus taeda wood properties by near infrared spectroscopy. Part 2: Whole-tree wood property maps. *Appita Journal*, **62** (3), 232-238.

Muneri, A. and Raymond, C.A. 2001 Nondestructive sampling of Eucalyptus globulus and E. nitens for wood properties; II. Fibre length and coarseness. *Wood Science and technology*, **35** (1-2), 41-56.

Murphy, T. 2008 *Evaluating Log Stiffness Using Acoustic Technology for Manufacturing Structural Oriented Strand Board.* Master, University of Georgia.

Naes, T., Isaksson, T., Fearn, T. and Davies, T. 2002 *A user-friendly guide to Multivariate Calibration and Classification*. NIR publications.

Nilsson, U. and Allen, H.L. 2003 Short-and long-term effects of site preparation, fertilization and vegetation control on growth and stand development of planted loblolly pine. *Forest Ecology and Management*, **175** (1), 367-377.

Niskanen, K. 1998 *Paper Physics*. TAPPI Press.

Paavilainen, L. 1993 Importance of Cross-Dimensional Fibre Properties and Coarseness for the Characterisation of Softwood Sulphate Pulp. *Paperi ja Puu*, **75** (5), 343-351.

Panshin, A. and DeZeeuw, C. 1980 Textbook of Wood Technology. McGraw-Hill, New York.

Pienaar, L. and Shiver, B. 1993 Early Results from an Old-Field Loblolly Pine Spacing Study in the Georgia Piedmont with Competition Control. *Southern Journal of Applied Forestry*, **17** (4), 193-196.

Pot, D., Chantre, G., Rozenberg, P., Rodrigues, J.C., Jones, G.L., Pereira, H. *et al.* 2002 Genetic control of pulp and timber properties in maritime pine (Pinus pinaster Ait.). *Annals of Forest Science*, **59** (5-6), 563-575.

Pulkkinen, I., Ala-Kaila, K. and Aittamaa, J. 2006 Characterization of wood fibers using fiber property distributions. *Chemical Engineering and Processing: Process Intensification*, **45** (7), 546-554.

R Development Core Team. 2016 R: A Language and Environment for Statistical Computing. 3.1.0 Ed., R Foundation for Statistical Computing, Vienna, Austria.

Raymond, C.A. and Schimleck, L.R. 2002 Development of near infrared reflectance analysis calibrations for estimating genetic parameters for cellulose content in Eucalyptus globulus. *Canadian Journal of Forest Research*, **32** (1), 170-176.

Roth, B.E., Li, X., Huber, D.A. and Peter, G.F. 2007 Effects of management intensity, genetics and planting density on wood stiffness in a plantation of juvenile loblolly pine in the southeastern USA. *Forest Ecology and Management*, **246** (2), 155-162.

RStudio Team. 2016 RStudio: Integrated Development for R. RStudio, Inc., . Boston, MA.

Savitzky, A. and Golay, M.J. 1964 Smoothing and Differentiation of Data by Simplified Least Squares Procedures. *Analytical chemistry*, **36** (8), 1627-1639.

Schimleck, L., Evans, R. and Ilic, J. 2001 Application of near infrared spectroscopy to a diverse range of species demonstrating wide density and stiffness variation. *IAWA Journal*, **22** (4), 415-429.

Schimleck, L.R., David Jones, P., Clark, A. and Peter, G.F. 2005 Near infrared spectroscopy for the nondestructive estimation of clear wood properties of Pinus taeda L. from the southern United States. *Forest Product Journal*, **55** (12), 21-28.

Schimleck, L.R. and Evans, R. 2004 Estimation of Pinus radiata D. Don tracheid morphological characteristics by near infrared spectroscopy. *Holzforschung*, **58** (1), 66-73.

Schimleck, L.R. and French, J. 2002 Application of NIR spectroscopy to clonal Eucalyptus globulus samples covering a narrow range of pulp yield. *Appita journal*, **55** (2), 149-154.

Schimleck, L.R., Jones, D.P., F., P.G., Daniels, R.F. and Clark, A. 2004 Nondestructive estimation of tracheid length from sections of radial wood strips by near infrared spectroscopy. *Holzforschung*, **58**, 375-381.

Schimleck, L.R., Kube, P.D., Raymond, C.A., Michell, A.J. and French, J. 2006 Extending Near Infrared Reflectance (NIR) Pulp Yield Calibrations to NewSites and Species. *J. Wood Chem. Technol.*, **26** (4), 299-311.

Schimleck, L.R., Mora, C. and Daniels, R.F. 2003 Estimation of the physical wood properties of green Pinus taedaradial samples by near infrared spectroscopy. *Canadian Journal of Forest Research*, **33** (12), 2297-2305.

Schimleck, L.R., Mora, C. and Daniels, R.F. 2004 Estimation of Tracheid Morphological Characteristics of Green Pinus taeda L. Radial Strips by Near Infrared Spectroscopy. *Wood and Fiber Science*, **36** (4), 527-535.

Schimleck, L.R., Stürzenbecher, R., Jones, D.P. and Evans, R. 2004 Development of wood property calibrations using near infrared spectra having different spectral resolutions. *Journal of Near Infrared Spectroscopy*, **12**, 1-7.

Schultz, R.P. 1997 *Loblolly Pine: The Ecology and Culture of loblolly pine (Pinus taeda L.)*. U.S. Department of Agriculture, Forest Service.

Schultz, R.P. 1999 Loblolly—the pine for the twenty-first century. In *Planted Forests: Contributions to the Quest for Sustainable Societies*, Springer, pp. 71-88.

Seth, R., Jang, H., Chan, B. and Wu, C. 1996 Transverse dimensions of wood pulp fibres and their implications for end use. Research report PRR 1231. Pulp and paper research institute of Canada, Montréal.

Sewell, M., Bassoni, D., Megraw, R., Wheeler, N. and Neale, D. 2000 Identification of QTLs influencing wood property traits in loblolly pine (Pinus taeda L.). I. Physical wood properties. *Theoretical and Applied Genetics*, **101** (8), 1273-1281.

Signal Developers. 2013 Package "signal".

Smook, G.A. 2002 *Handbook for Pulp & Paper Technologists*. Vancouver: Angus Wilde Publications.

Snee, R.D. 1977 Validation of Regression Models: Methods and Examples. *Technometrics*, **19** (4), 415-428.

Stanturf, J., Madsen, P. and Lamb, D. 2012 *A Goal-Oriented Approach to Forest Landscape Restoration*. Springer Science & Business Media.

Stevens, A. and Ramirez–Lopez, L. 2014 An introduction to the prospectr package.

Stokke, D.D. and Groom, L.H. 2008 *Characterization of the Cellulosic Cell Wall*. John Wiley & Sons.

Therneau, T.M., Atkinson, E.J. and Ripley, B. 2015 An introduction to recursive partitioning using the RPART routines. Technical Report 61. URL http://www.mayo.edu/hsr/techrpt/61.pdf.

Trincado, G., VanderSchaaf, C.L. and Burkhart, H.E. 2007 Regional mixed-effects height–diameter models for loblolly pine (Pinus taeda L.) plantations. *European Journal of Forest Research*, **126** (2), 253-262.

Tsuchikawa, S. 2007 A Review of Recent Near Infrared Research for Wood and Paper. *Applied Spectroscopy Reviews*, **42** (1), 43-71.

Tsuchikawa, S. and Schwanninger, M. 2013 A Review of Recent Near Infrared Research for Wood and Paper (Part 2). *Applied Spectroscopy Reviews*, **48** (1), 560-587.

van Leeuwen, M., Hilker, T., Coops, N.C., Frazer, G., Wulder, M.A., Newnham, G.J. *et al.* 2011 Assessment of standing wood and fiber quality using ground and airborne laser scanning: A review. *Forest Ecology and Management*, **261** (9), 1467-1478.

Verrill, S.P., Kretschmann, D.E., Herian, V.L., Wiemann, M.C. and Alden, H.A. 2011 Concerns About a Variance Approach to X-Ray Diffractometric Estimation of Microfibril Angle in Wood. *Wood and fiber science*, **43** (2), 153.

Via, B.K. 2004 *Modeling Lingleaf Pine (Pinus palustris mill) Wood Properties Using Near Infrared Spectroscopy.* Doctorate, Louisiana State University.

Via, B.K., Shupe, T.F., Groom, L.H., Stine, M. and So, C.-L. 2003 Multivariate modelling of density, strength and stiffness from near infrared spectra for mature, juvenile and pith wood of longleaf pine (Pinus palustris). *Journal of near infrared spectroscopy*, **11** (5), 365-378.

Via, B.K., Shupe, T.F., Stine, M., So, C.-L. and Groom, L.H. 2005 Tracheid length prediction in Pinus palustris by means of near infrared spectroscopy: the influence of age. *Holz als Roh- und Werkstoff*, **63** (3), 231-236.

Via, B.K., So, C.-L., Shupe, T.F., Stine, M. and Groom, L.H. 2005 Ability of Near Infrared Spectroscopy to Monitor Air-Dry Density Distribution and Variation of Wood. *Wood and Fiber Science*, **3** (3), 394-402.

Wang, T. and Aitken, S.N. 2001 Variation in xylem anatomy of selected populations of lodgepole pine. *Canadian Journal of Forest Research*, **31** (11), 2049-2057.

Wang, X. 2003 *Modeling Changes in Strength and Stiffness of Loblolly Pine Wood.* Master, University of Georgia.

Wathén, R. 2006 *Studies on Fiber Strength and its Effect on Paper Properties.* Doctor of Science in Technology, Helsinki University of Technology.

Wear, D.N. and Greis, J.G. 2002 Southern Forest Resource Assessment: Summary of Findings. *Journal of Forestry*, **100** (7), 6-14.

White, D.E., Courchene, C., McDonough, T., Schimleck, L., Jones, D., Purnell, R. *et al.* 2009 Effects of specific gravity and wood chemical content on the pulp yield of loblolly pine. *TAPPI Journal*, **92** (4), 29-34.

Williams, C.G. and Megraw, R.A. 1994 Juvenile-mature relationships for wood density in Pinus taeda. *Canadian Journal of Forest Research*, **24** (4), 714-722.

Williams, P.C. and Sobering, D. 1993 Comparison of commercial near infrared transmittance and reflectance instruments for analysis of whole grains and seeds. *Journal of Near Infrared Spectroscopy*, **1** (1), 25-32.

Xu, P., Donaldson, L., Walker, J., Evans, R. and Downes, G. 2004 Effects of density and microfibril orientation on the vertical variation of low-stiffness wood in radiata pine butt logs. *Holzforschung*, **58** (6), 673-677.

Yang, Z., Li, K., Zhang, M., Xin, D. and Zhang, J. 2016 Rapid determination of chemical composition and classification of bamboo fractions using visible–near infrared spectroscopy coupled with multivariate data analysis. *Biotechnology for biofuels*, **9** (1), 1.

Yeh, T.-F., Chang, H.-m. and Kadla, J.F. 2004 Rapid prediction of solid wood lignin content using transmittance near-infrared spectroscopy. *Journal of Agricultural and Food Chemistry*, **52** (6), 1435-1439.

Zhao, D., Kane, M. and Borders, B.E. 2011 Growth responses to planting density and management intensity in loblolly pine plantations in the southeastern USA Lower Coastal Plain. *Annals of Forest Science*, **68** (3), 625-635.

Ziegel, E.R. 2004 A User-Friendly Guide to Multivariate Calibration and Classification. *Technometrics*, **46** (1).

Zobel, B. 1961 Some effects of fertilizers on wood properties of loblolly pine. *TAPPI*, **44**, 186-192.

Zobel, B.J. and Van Buijtenen, J.P. 1989 *Wood Variation: Its Causes and Control*. Springer-Verlag.